

## Senolytic vaccination improves normal and pathological age-related phenotypes and increases lifespan in progeroid mice

Masayoshi Suda<sup>1,14</sup>, Ippei Shimizu<sup>1,14</sup>, Goro Katsuumi <sup>1,14</sup>, Yohko Yoshida<sup>1</sup>, Yuka Hayashi<sup>2</sup>, Ryutaro Ikegami<sup>2</sup>, Naomi Matsumoto<sup>3</sup>, Yutaka Yoshida<sup>4</sup>, Ryuta Mikawa <sup>1,5</sup>, Akihiro Katayama<sup>6</sup>, Jun Wada <sup>1,6</sup>, Masahide Seki <sup>1,6</sup>, Yutaka Suzuki <sup>1,6</sup>, Atsushi Iwama <sup>1,6</sup>, Hironori Nakagami <sup>1,6</sup>, Ayako Nagasawa <sup>1,6</sup>, Ryuichi Morishita <sup>1,6</sup>, Masataka Sugimoto<sup>5</sup>, Shujiro Okuda <sup>1,6</sup>, Masanori Tsuchida <sup>1,6</sup>, Kazuyuki Ozaki<sup>2</sup>, Mayumi Nakanishi-Matsui<sup>3</sup> and Tohru Minamino <sup>1,6</sup>, <sup>1,2</sup>

Elimination of senescent cells (senolysis) was recently reported to improve normal and pathological changes associated with aging in mice<sup>1,2</sup>. However, most senolytic agents inhibit antiapoptotic pathways3, raising the possibility of offtarget effects in normal tissues. Identification of alternative senolytic approaches is therefore warranted. Here we identify glycoprotein nonmetastatic melanoma protein B (GPNMB) as a molecular target for senolytic therapy. Analysis of transcriptome data from senescent vascular endothelial cells revealed that GPNMB was a molecule with a transmembrane domain that was enriched in senescent cells (seno-antigen). GPNMB expression was upregulated in vascular endothelial cells and/or leukocytes of patients and mice with atherosclerosis. Genetic ablation of Gpnmb-positive cells attenuated senescence in adipose tissue and improved systemic metabolic abnormalities in mice fed a high-fat diet, and reduced atherosclerotic burden in apolipoprotein E knockout mice on a highfat diet. We then immunized mice against Gpnmb and found a reduction in Gpnmb-positive cells. Senolytic vaccination also improved normal and pathological phenotypes associated with aging, and extended the male lifespan of progeroid mice. Our results suggest that vaccination targeting seno-antigens could be a potential strategy for new senolytic therapies.

It has been demonstrated that senescent cells accumulate in various tissues with aging or in response to metabolic stress<sup>4,5</sup>. For example, senescent vascular endothelial cells are observed in human atherosclerotic plaque<sup>6</sup>. Senescent vascular endothelial cells exhibit functional abnormalities, such as impairment of endothelium-dependent vasodilation, and these cells also produce inflammatory

molecules known as senescence-associated secretary phenotype (SASP) factors<sup>7</sup>. Both of these changes accelerate the development of atherosclerosis<sup>7</sup>. Visceral adipose tissue develops senescence-like features in patients with type 2 diabetes and promotes insulin resistance by production of inflammatory adipokines<sup>8</sup>. In mice, specific deletion of the p53/p21 pathway in vascular tissue or adipose tissue prevents the onset of atherosclerosis and diabetes, respectively, suggesting that inhibition of this pathway could potentially be a strategy for management of age-associated diseases<sup>7,9</sup>. However, direct inhibition of the p53/p21 pathway could increase the risk of carcinogenesis, so another approach to antisenescence therapy is required.

It was reported that elimination of p16<sup>Ink4a</sup>-positive senescent cells delayed tumorigenesis, improved age-associated pathologies, and extended the median lifespan of middle-aged wild-type (WT) mice1, indicating that age-associated accumulation of senescent cells contributes to pathological aging and that elimination of senescent cells (senolysis or senolytic therapy) could be an attractive strategy for antisenescence therapy without the risk of promoting cancer. Conversely, transplantation of a small population of senescent cells into young mice caused persistent physical dysfunction and shortened their healthy lifespan2. Several senolytic agents have been shown to improve age-associated pathologies and diseases reversibly and extend the healthy lifespan in aged mice<sup>3</sup>. While substantial progress has been made in senolytic therapy, concerns remain regarding the safety and specificity of the senolytics reported on to date. Because senescent cells are heterogeneous, we need to develop more cell or tissue-specific treatments that efficiently eliminate unwanted cells without affecting the beneficial role of these cells in processes such as tissue repair.

Department of Cardiovascular Biology and Medicine, Juntendo University Graduate School of Medicine, Tokyo, Japan. <sup>2</sup>Department of Cardiovascular Biology and Medicine, Niigata University Graduate School of Medical and Dental Sciences, Niigata, Japan. <sup>3</sup>Division of Biochemistry, School of Pharmacy, Iwate Medical University, Iwate, Japan. <sup>4</sup>Department of Structural Pathology, Kidney Research Center, Niigata University Graduate School of Medical and Dental Sciences, Niigata, Japan. <sup>5</sup>Research Institute, National Center for Geriatrics and Gerontology, Aichi, Japan. <sup>6</sup>Department of Nephrology, Rheumatology, Endocrinology and Metabolism, Okayama University Graduate School of Medicine, Dentistry and Pharmaceutical Sciences, Okayama, Japan. <sup>7</sup>Department of Computational Biology and Medical Sciences, Graduate School of Frontier Sciences, The University of Tokyo, Chiba, Japan. <sup>8</sup>Division of Stem Cell and Molecular Medicine, Center for Stem Cell Biology and Regenerative Medicine, The Institute of Medical Science, The University of Tokyo, Tokyo, Japan. <sup>9</sup>Department of Health Development and Medicine, Graduate School of Medicine, Osaka University, Osaka, Japan. <sup>10</sup>Department of Thoracic and Cardiovascular Surgery, Niigata University Graduate School of Medical and Dental Sciences, Niigata, Japan. <sup>11</sup>Department of Clinical Gene Therapy, Osaka University Graduate School of Medical Research and Development-Core Research for Evolutionary Medical Science and Technology (AMED-CREST), Japan Agency for Medical Research and Development, Tokyo, Japan. <sup>14</sup>These authors contributed equally: Masayoshi Suda, Ippei Shimizu, Goro Katsuumi. <sup>58</sup>e-mail: t.minamino@juntendo.ac.jp

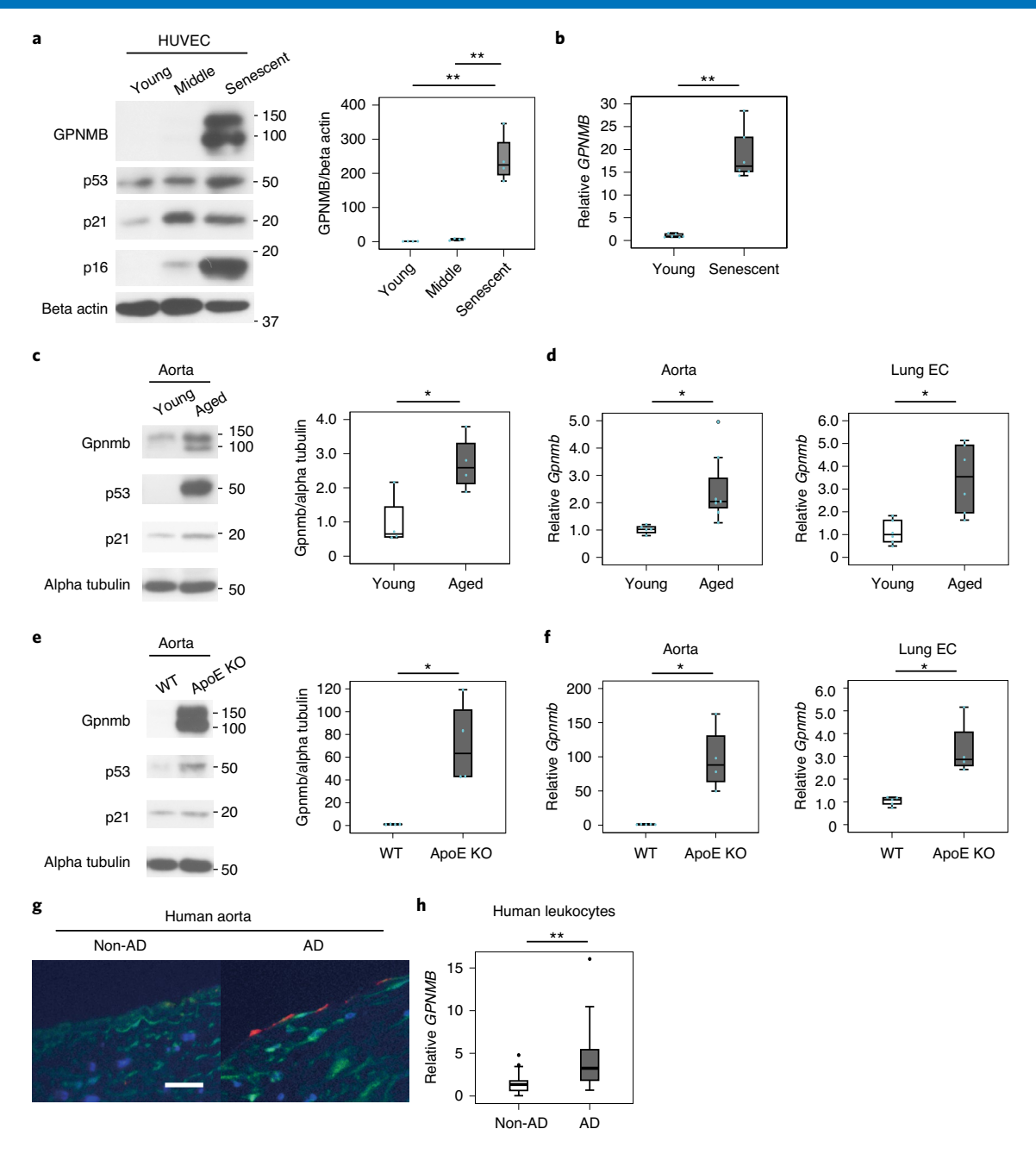


**Fig. 1 | GPNMB** is a potential candidate of seno-antigen. **a**, Western blot analysis in young (passage 4, n=4), middle-aged (passage 14, n=4) and replicative senescent HUVECs (passage 18, n=4). **b**, *GPNMB* expression in young HUVECs (passage 6, n=6) and replicative senescent HUVECs (passage 17, n=6). **c**, Western blot analyses in the aortas of young mice (12 weeks old, n=4) and aged mice (109–110 weeks old, n=4). **d**, qPCR analysis of relative *Gpnmb* expression in the aortas and lung endothelial cells (ECs) of young mice (12 weeks old) and aged mice (109–110 weeks old) (aorta, n=5 for young mice and n=7 for aged mice; endothelial cells, n=6 for young mice and n=6 for aged mice). **e**, Western blot analysis in the aortas of WT mice (n=4) and ApoE KO mice (n=4). Mice were fed an HFD for 12 weeks (from 4 weeks to 16 weeks old) and then were analyzed. **f**, qPCR analysis of relative *Gpnmb* expression in the aortas and lung endothelial cells of WT mice and ApoE KO mice (aorta, n=5 for WT mice and n=4 for ApoE mice). **g**, Immunohistochemistry for GPNMB (red) in the aortas of patients with or without atherosclerotic disease (AD). Vascular endothelial cells were stained with isolectin IB4 (green) and nuclei were labeled with Hoechst (blue). Representative photomicrographs from three independent experiments with different patients are shown at x1200 magnification. Scale bar,  $25 \, \mu$ m. **h**, qPCR analysis of *GPNMB* expression in leukocytes of patients with or without atherosclerotic disease (n=24 for non-AD and n=46 for AD). Two outlier values (not shown in the graph) were detected in the atherosclerotic disease group by boxplot analysis and were excluded from statistical assessment. The data were analyzed by one-way ANOVA, followed by Tukey's multiple comparison test (**a**) or by the two-tailed Student's t-test (**b-f** and **h**), t-20.05, t-70.1. The data are shown as box and whisker plots that display the range of the data (whiskers), the 25th and 75th percentiles (b

#### Results

**GPNMB is a candidate seno-antigen.** To develop a more specific senolytic therapy with fewer off-target effects, we adopted an approach based on targeting seno-antigens specifically expressed

by senescent cells. We used transcriptome data from senescent human vascular endothelial cells to search for molecules with transmembrane domains because this approach would allow us to develop a new therapeutic strategy that could eliminate senescent

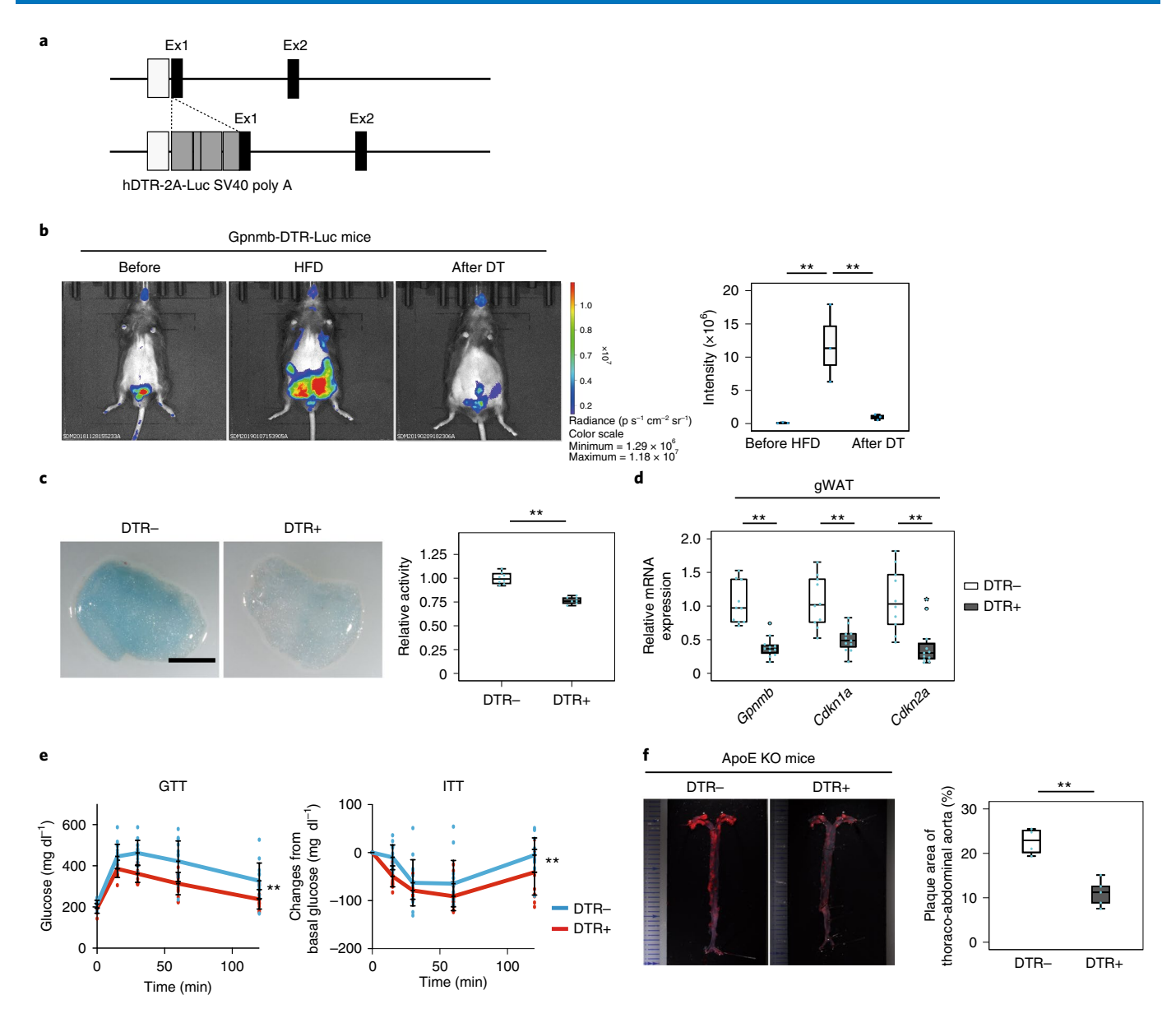


**Fig. 2 | Elimination of Gpnmb-positive cells attenuates metabolic abnormalities and atherosclerosis in mice fed a HFD. a**, Schematic drawing of the strategy for generation of Gpnmb-DTR-luciferase (Luc) mice. **b**, Luciferase activity was monitored by an IVIS in Gpnmb-DTR-luciferase mice before starting an HFD (left: before, 6 weeks old), after 6 weeks on the HFD (middle: HFD, 12 weeks old), and after intraperitoneal injection of DT (right: after DT, 16 weeks old). The right graph shows the quantification of luciferase activity (n=3 each). **c**, SA-beta-gal assay of visceral adipose tissue obtained from Gpnmb-DTR-luciferase mice (DTR+) or littermate controls (DTR-) on the HFD treated with DT. The right graph displays quantification of SA-beta-gal activity (n=8 for DTR- and n=7 for DTR+). Scale bar, 5 mm. **d**, qPCR analysis of relative *Gpnmb* expression and senescence markers in visceral adipose tissue obtained from Gpnmb-DTR-luciferase mice (DTR+) or littermate controls (DTR-) mice on the HFD treated with DT (n=10 for DTR- and n=11 for DTR+). **e**, Glucose tolerance test (GTT; left) and insulin tolerance test (ITT; right) in Gpnmb-DTR-luciferase mice (DTR+) or littermate controls (DTR-) on the HFD treated with DT (at 12 weeks old). Mice were examined at 13 weeks old (GTT, n=14 each; ITT, n=14 for DTR- and n=13 for DTR+). Changes from basal glucose levels are shown in the ITT graph. **f**, Oil Red O-stained thoraco-abdominal aortas of ApoE KO/Gpnmb-DTR-luciferase mice (DTR+) or ApoE KO/Gpnmb-DTR-luciferase littermate controls (DTR- on the HFD treated with DT. The right graph shows quantification of the plaque area in the thoraco-abdominal aorta (n=4 for DTR- and n=5 for DTR+). The data were analyzed by one-way ANOVA followed by Tukey's multiple comparison test (**b**), the two-tailed Student's *t*-test (**c**, **d** and **f**) or repeated measures analysis (**e**), \*P<0.05, \*P<0.05, \*P<0.01. The data are shown as box and whisker plots that display the range of the data (whiskers), the 25th and 75th p

cells through antibody-dependent cellular cytotoxicity (ADCC) by targeting a seno-antigen. Gene expression profiles for GSE37091 and GSE13712 were analyzed with the GEO2R analysis tool provided as a web service in the Gene Expression Omnibus database<sup>10</sup>. Genes showing threefold or greater upregulation in senescent samples in comparison to young samples were extracted. The pres-

ence or absence of transmembrane regions was predicted with TMHMM2.0 for protein sequences downloaded from the KEGG GENES database (2 May 2014 version)<sup>11,12</sup>; this process identified ten genes with predicted transmembrane regions (Supplementary Table 1). From among these genes, we selected *GPNMB* as a candidate seno-antigen gene because evidence is available for a potential

link between GPNMB and human aging<sup>13</sup>. We found a marked increase of GPNMB expression in human umbilical vein endothelial cells (HUVECs) undergoing replicative senescence (Fig. 1a,b). We also found significant upregulation of Gpnmb expression in the aortas and isolated endothelial cells of aged mice, apolipoprotein E (ApoE) knockout (KO) mice and mice on a high-fat diet (HFD), and showed that this upregulation was associated with increased expression of senescence markers, such as p53 and p21 (Fig. 1c-f and Extended Data Fig. 1a). Furthermore, upregulation of Gpnmb was identified in other tissues of aged mice, such as the lung, visceral fat (gonadal white adipose tissue; gWAT), and bone marrow, as well as in the visceral fat of HFD-fed mice (Extended Data Fig. 1b,c). Moreover, histological examination revealed upregulation of GPNMB expression in vascular endothelial cells from patients with atherosclerosis, but not in cells from patients without atherosclerosis (Fig. 1g). Likewise, GPNMB expression was significantly increased in leukocytes from patients with atherosclerosis compared to leukocytes from patients without atherosclerosis (Fig. 1h and Extended Data Fig. 1d). These results suggested that Gpnmb could be a molecular target for senolytic therapy.

Effects of genetic elimination of Gpnmb-positive cells. To test the possibility of using GPNMB as a molecular target for senolytic therapy, we established a transgenic mouse model in which the diphtheria toxin receptor (DTR; human HB-EGF I117V/L148V) and luciferase were expressed at the Gpnmb locus (Gpnmb-DTRluciferase mice) (Fig. 2a), allowing us to detect Gpnmb-positive cells by monitoring luciferase activity and to eliminate these cells by administration of diphtheria toxin (DT). Gpnmb-DTRluciferase mice were maintained on the HFD from 4 to 16 weeks of age with intraperitoneal injection of DT (50 µg kg<sup>-1</sup> body weight) at 12 and 14 weeks. Consistent with our western blot analysis of Gpnmb expression in visceral fat from HFD mice (Extended Data Fig. 1c), strong luciferase signals were detected in the abdomen when Gpnmb-DTR-luciferase mice were analyzed at 16 weeks (Fig. 2b). Conversely, administration of DT reduced abdominal luciferase activity, and this reduction was associated with improvement of the senescence-like changes in visceral adipose tissue, as demonstrated by a decrease of senescence-associated beta-galactosidase (SA-beta-gal) activity and by downregulation of Cdkn2a and Cdkn1a expression (Fig. 2b-d). Deletion of Gpnmb-positive cells also significantly improved metabolic abnormalities induced by the HFD (Fig. 2e). Moreover, we established Gpnmb-DTR-luciferase mice with an ApoE KO background. These mice were fed the HFD from 4 weeks of age, treated with DT at 12 weeks and 14 weeks, and analyzed at 16 weeks. We found that deletion of Gpnmb-positive cells significantly reduced the atherosclerotic plaque burden (Fig. 2f), providing further evidence that Gpnmb was a possible target for senolytic therapy.

Effects of Gpnmb vaccination on metabolic abnormality. We then sought to develop a peptide vaccine for Gpnmb. To create a vaccine, we chose two peptide sequences (A, RRGDGRWKD; and B, RSQHLRFPDR) from the extracellular domain of Gpnmb, and, to elicit production of specific antibodies, we generated peptides conjugated with the immunogenic carrier protein keyhole limpet hemocyanin (KLH). Equal volumes of a KLH-conjugated antigenic peptide and a water-in-oil adjuvant were emulsified and injected subcutaneously for immunization. The antibody titer against Gpnmb was higher with the vaccine containing peptide A (Extended Data Fig. 2a), so this vaccine was used for all experiments reported here. Western blot analysis of conditioned medium obtained from cultured splenocytes of Gpnmb-vaccinated mice detected specific signals for Gpnmb expression by senescent cells in the stromal vascular fraction (SVF) from WT mice but not in the SVF from Gpnmb KO mice (Extended Data Fig. 2b). We subsequently confirmed that antibodies obtained from Gpnmb-vaccinated mice showed ADCC that was mediated by natural killer (NK) cells in a dose-dependent manner and that these NK cells specifically targeted senescent SVF cells that expressed Gpnmb (Extended Data Fig. 2c).

We then looked at the potential for GPNMB vaccination to mitigate metabolic abnormalities in HFD mice. WT mice were fed the HFD from 4 weeks of age and were immunized by subcutaneous injection of Gpnmb vaccine at 8 weeks of age, followed by analysis at 16 weeks. Administration of Gpnmb vaccine reduced Gpnmb expression and the associated luciferase activity in visceral adipose tissue (Fig. 3a-c), indicating that this vaccine eliminated Gpnmbpositive cells. Administration of Gpnmb vaccine also attenuated the increase of p19Arf-dependent luciferase activity<sup>14</sup> (Fig. 3d), significantly ameliorated senescence-like phenotypic changes in visceral adipose tissue (the increase of SA-beta-gal activity and upregulation of negative cell cycle regulators) (Fig. 3b,e,f), and improved the metabolic profile compared with administration of a control vaccine (Fig. 3g). However, these effects were not observed when Gpnmb KO mice were administered the Gpnmb vaccine (Fig. 3h-i), indicating that the response to vaccination was mediated by Gpnmb. Moreover, the beneficial impacts of Gpnmb vaccination were attenuated when the vaccinated mice were treated with a neutralizing antibody against NK or CD8+ T cells, indicating that NK and CD8+ T cells are crucial for the effects of Gpnmb vaccination in vivo (Fig. 3k and Extended Data Fig. 2d).

FACS analysis with SPiDER-beta-gal in the SVF of visceral adipose tissue from HFD-fed mice showed that about 90% of the Gpnmb-positive (Gpnmb<sup>high</sup>) cells had high SA-beta-gal activity, indicating that they were senescent cells (Extended Data Fig. 2e,f). We also found that Gpnmb was mainly expressed by endothelial cells (CD31<sup>+</sup> CD45<sup>-</sup>) and CD31<sup>-</sup> CD45<sup>-</sup> cells (most likely fibroblasts) and to a lesser extent by hematopoietic cells (CD31<sup>-</sup> CD45<sup>+</sup>), including macrophages (CD45<sup>+</sup> CD14<sup>+</sup> Ly6g<sup>-</sup> F4/80<sup>+</sup>) and T cells (CD45<sup>+</sup> Cd11<sup>-</sup>

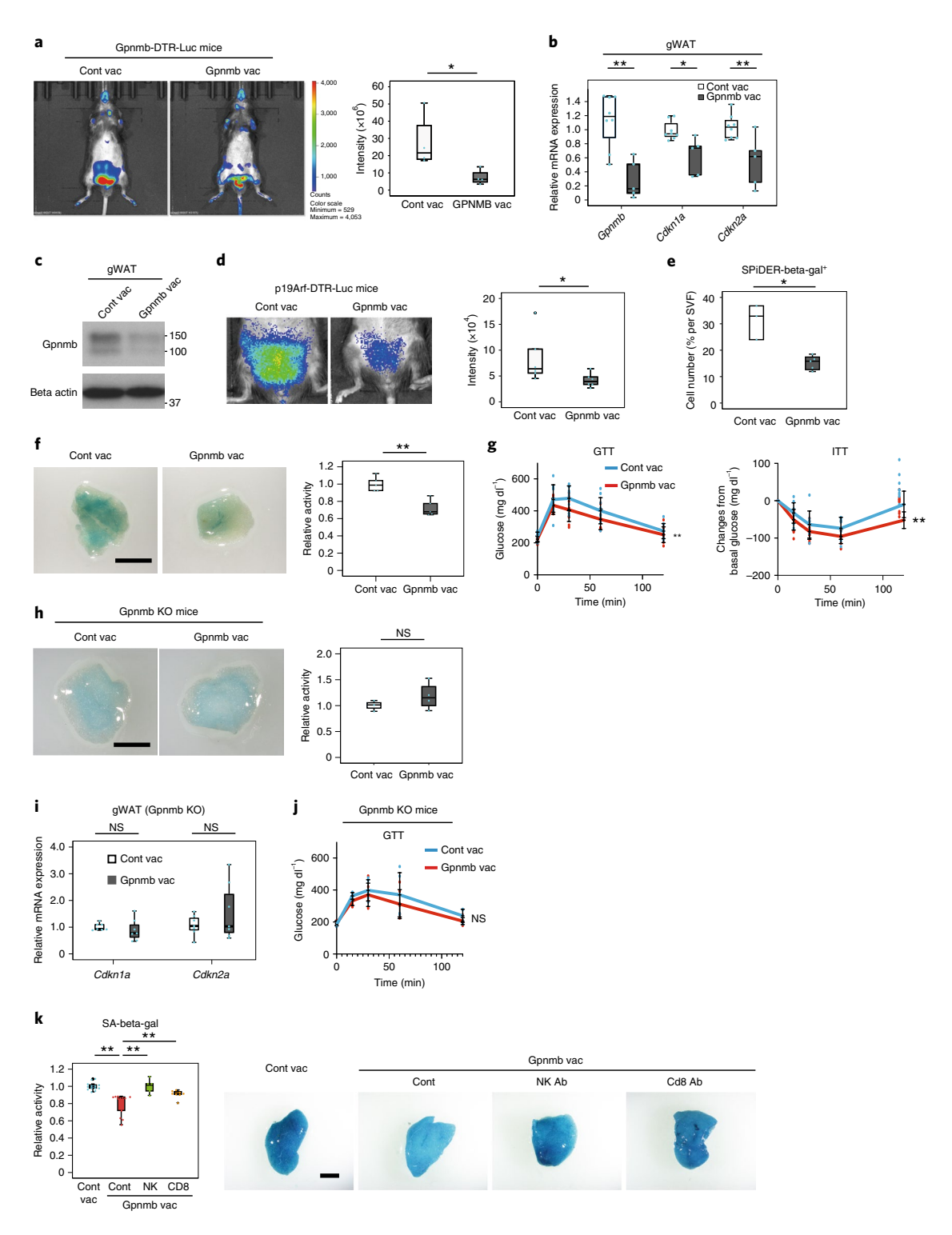
**Fig. 3 | Gpnmb vaccination improves HFD-induced metabolic abnormalities. a**, Luciferase activity in Gpnmb-DTR-luciferase mice on the HFD treated with Gpnmb vaccine (Gpnmb vac, n=4) or control vaccine (Cont vac, n=4). **b**, Relative expression of *Gpnmb* and senescence markers in visceral adipose tissue (Cont vac, n=8; Gpnmb vac, n=5). **c**, Western blot analysis in visceral adipose tissue from the Gpnmb vac and Cont vac groups. The similar results were obtained from three independent experiments. **d**, Luciferase activity in p19<sup>ARF</sup>-DTR-luciferase mice (Cont vac, n=5; Gpnmb vac, n=6). One outlier value was detected in the control vaccine group by boxplot analysis and was excluded from statistical assessment. **e**, Fluorescence-assisted cell sorting (FACS) analysis with SPiDER-beta-gal to assess the SVF (Cont vac, n=3; Gpnmb vac, n=5). **f**, SA-beta-gal assay of visceral adipose tissue obtained (Cont vac, n=5). Scale bar, 5 mm. **g**, GTT (left) and ITT (right) (GTT, n=10 for Cont vac and n=11 for Gpnmb vac; ITT, n=9 for Cont vac and n=10 for Gpnmb vac). Changes from basal glucose levels are shown in the ITT graph. **h**, SA-beta-gal assay of visceral adipose tissue obtained from Gpnmb KO mice (Cont vac, n=3; Gpnmb vac, n=4). Scale bar, 5 mm. **i**, Relative expression of senescence makers in visceral adipose tissue from Gpnmb KO mice (Cont vac, n=7; Gpnmb vac, n=7). **j**, GTT of Gpnmb KO mice (Cont vac, n=6). **k**, Effects of a neutralizing antibody on SA-beta-gal activity of visceral adipose tissue. Scale bar, 5 mm. (n=13, 14, 6 and 8 for Cont vac, Gpnmb vac + Cont, Gpnmb vac + NK and Gpnmb vac + CD8). The data were analyzed by the two-tailed Student's t-test (**a**, **b**, **d-f**, **h** and **i**), univariate analysis of variance (**g**), repeated measures (**j**) or one-way ANOVA followed by Tukey's multiple comparison test (**k**). \*P < 0.05; \* $^*P < 0.05$ ; \* $^*D < 0.05$ ; N, not significant. The data are shown as box and whisker plot

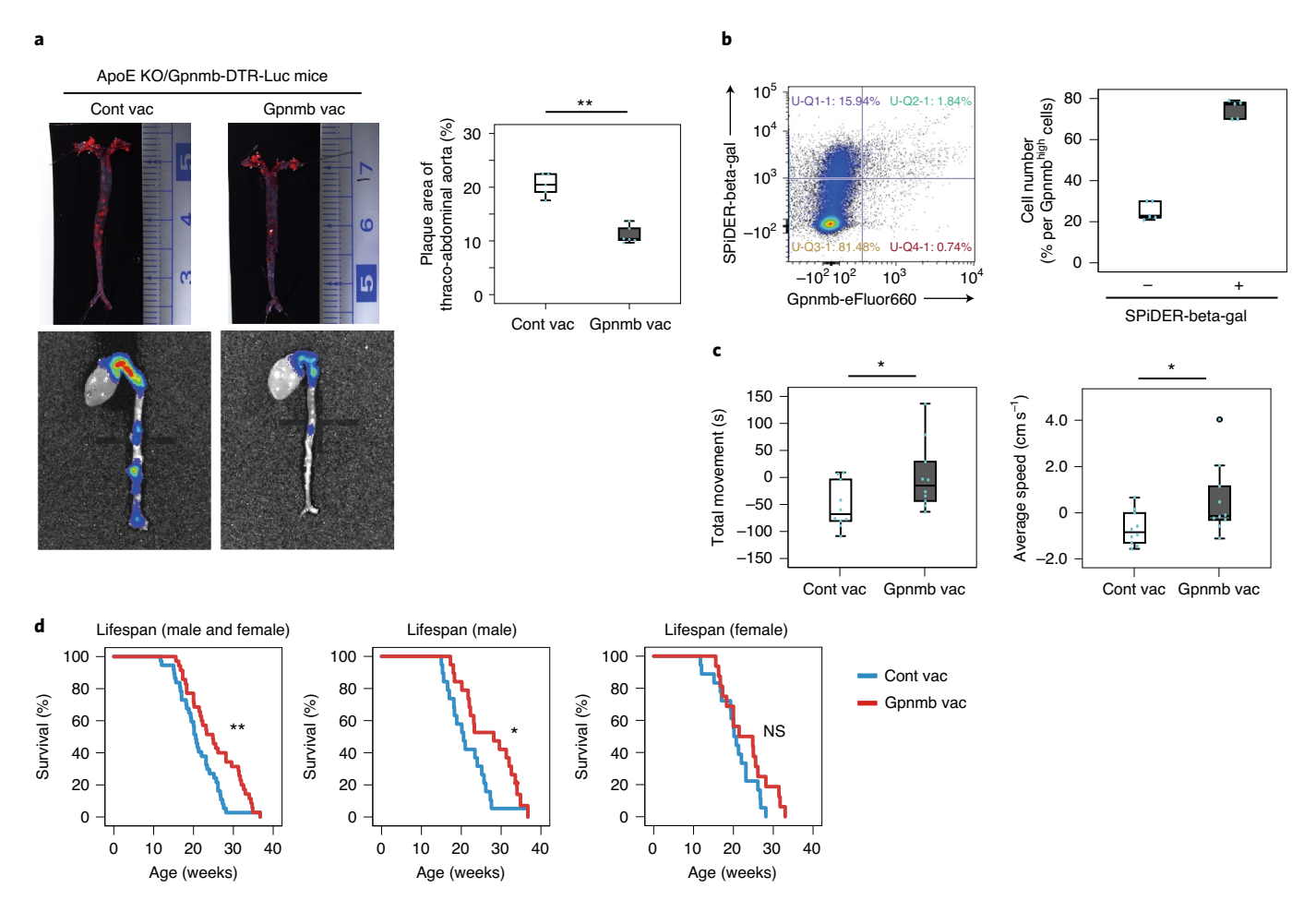
NATURE AGING I www.nature.com/nataging

CD3<sup>+</sup>) (Extended Data Fig. 2g). FACS analyses revealed that Gpnmb vaccination eliminated Gpnmb-positive endothelial cells (Gpnmb<sup>high</sup> CD31<sup>+</sup> CD45<sup>-</sup>) and Gpnmb-positive nonendothelial/hematopoietic cells (Gpnmb<sup>high</sup> CD31<sup>-</sup> CD45<sup>-</sup>) with high SA-beta-gal activity from visceral adipose tissue of HFD-fed mice but not Gpnmb<sup>low</sup> cells with low SA-beta-gal activity (Extended Data Fig. 2h,i).

Effects of Gpnmb vaccination on aging phenotypes. In another experiment, we fed the HFD to ApoE KO mice from 4 weeks of age, administered Gpnmb vaccine at 8 weeks of age, and analyzed

these mice at 16 weeks. We demonstrated that administration of the Gpnmb vaccine significantly reduced atherogenesis and decreased Gpnmb-dependent luciferase activity in the aorta compared with a control vaccine (Fig. 4a). Aortic expression of pro-inflammatory molecules was downregulated by Gpnmb vaccination along with decreased expression of *Gpnmb* and negative cell cycle regulators (Extended Data Fig. 3a). Administration of Gpnmb vaccine did not affect body weight (Extended Data Fig. 3b). FACS analyses with SPiDER-beta-gal in the aorta of ApoE KO mice showed that about 70% of Gpnmb-positive cells had high SA-beta-gal activity,





suggesting that they had likely undergone cellular senescence (Fig. 4b). We also found that Gpnmb-positive cells (Gpnmb<sup>high</sup>) were mainly detected in endothelial (CD31+ CD45-) and CD31- CD45cell populations (most likely fibroblasts and smooth muscle cells) and to a lesser extent in hematopoietic cells (CD31- CD45+), including macrophages (CD45+ CD14+ Ly6g- F4/80+) (Extended Data Fig. 3c). Gpnmb vaccination decreased SA-beta-gal activity in the aorta of ApoE KO mice, mainly eliminated Gpnmb-positive cells from endothelial (CD31+ CD45-) and hematopoietic cell populations (CD31- CD45+), including macrophages (CD45+ CD14+ Ly6g<sup>-</sup> F4/80<sup>+</sup>), and also modestly eliminated these cells from nonendothelial/hematopoietic cell populations (CD31 CD45) (Extended Data Fig. 3d,e), but did not decrease the amount of cells with low Gpnmb expression and low SA-beta-gal activity (Extended Data Fig. 3f). However, we could not exclude the possibility that elimination of senescent cells expressing low levels of Gpnmb or nonsenescent cells expressing high levels of Gpnmb contributed to the beneficial effects of Gpnmb vaccination.

To investigate the effect of vaccination on normal aging, we administered Gpnmb vaccine to middle-aged mice (50 weeks old) and examined their performance in the open field test before vaccination and 20 weeks after vaccination (70 weeks old). In the control group, both total movements and the average speed of movement decreased with age, but these age-associated changes were significantly ameliorated by Gpnmb vaccination (Fig. 4c). To investigate the effects of Gpnmb vaccine on the lifespan, we vaccinated Zmpste24 KO mice (a model of Hutchinson-Gilford progeria syndrome) at 10 weeks of age and evaluated their survival. In the control group, all of the mice died by 30 weeks of age. In contrast, mice, especially male mice, administered Gpnmb vaccine showed a better survival rate, even when the vaccine was administered at 10 weeks of age (Fig. 4d). Likewise, administration of Gpnmb vaccine significantly extended the median lifespan of Zmpste24 KO mice, especially male mice, compared with mice treated with control vaccine (male and female mice,  $21.1 \pm 0.85$  weeks versus  $25.3 \pm 1.10$  weeks (P < 0.01); male mice,  $21.7 \pm 1.27$  weeks versus  $27.1 \pm 1.53$  weeks

(P<0.01); female mice, 20.5  $\pm$  1.13 weeks versus 23.2  $\pm$  1.46 weeks (NS)) (Extended Data Fig. 3g).

Treatment with senolytics and dietary metabolic abnormalities. Over 20 agents, all of which selectively deplete senescent cells, have been identified<sup>3</sup>. Among them, the combination of two senolytic agents, dasatinib and quercetin (D+Q), has been shown to improve vasomotor function significantly in aged mice<sup>15</sup>, and alleviate obesity-induced metabolic dysfunction<sup>16</sup>. In addition, treatment with Navitoclax (ABT-263) has been shown to improve glucose metabolism and beta cell function while decreasing the expression of senescence markers and SASP factors<sup>17</sup>. The current study compared the effects of Gpnmb vaccination with D+Q and Navitoclax treatment in mice. In the Gpnmb vaccination group, WT mice were fed a HFD from 4 weeks of age and immunized with Gpnmb vaccine by subcutaneous injection at 8 weeks of age, followed by analysis at 16 and 24 weeks (Extended Data Fig. 4a). In the D+Q and Navitoclax groups, WT mice were fed a HFD from 4 weeks of age and administered senolytics or vehicle at 8 and 12 weeks of age by oral gavage for five consecutive days. The mice were analyzed at 16 and 24 weeks of age (Extended Data Fig. 4a). In all groups, there were no differences in body weight, food intake or energy expenditure (Extended Data Fig. 4b,c). When p19Arf-luciferase reporter mice were treated with D+Q or Navitoclax, the increase in p19Arf-dependent luciferase activity was attenuated in the abdomen (Extended Data Fig. 4d,e). Likewise, Gpnmb vaccination suppressed the increase of p19Arf-dependent luciferase activity, along with an increased titer of anti-Gpnmb antibody (Extended Data Fig. 4d-f). The senescencelike phenotypic changes in visceral adipose tissue (the increase of SA-beta-gal activity and upregulation of *Cdkn2a*) were improved in the D+Q and Navitoclax groups at 16 weeks of age; however, these beneficial effects declined at 24 weeks of age (Extended Data Fig. 4g,h). In contrast, Gpnmb vaccination consistently improved senescence-like phenotypic changes in visceral adipose tissue (Extended Data Fig. 4g,h). Treatment with D+Q or Navitoclax improved glucose intolerance, but insulin resistance developed at 24 weeks of

#### Discussion

ing time (Extended Data Fig. 4j).

We demonstrated that elimination of Gpnmb-positive cells by vaccination could improve HFD-induced atherogenesis and metabolic dysfunction in mice. Eliminating such cells also ameliorated normal and pathological aging in aged mice and prolonged the lifespan of mice with premature aging. These beneficial effects of vaccination are likely mediated by ADCC-dependent elimination of Gpnmb-positive cells, although other mechanisms might also be involved. Our results suggest that vaccination targeting Gpnmb could be a potential strategy for new senolytic therapies.

age (Extended Data Fig. 4i and Supplementary Fig. 1). In contrast,

the beneficial effects of Gpnmb vaccination on glucose metabolism

were sustained until 24 weeks of age (Extended Data Fig. 4i and

Supplementary Fig. 1). Finally, Navitoclax treatment significantly

reduced white blood cell and platelet counts and prolonged bleed-

GPNMB is a type I transmembrane protein that was originally identified in melanoma cell lines<sup>18</sup>. GPNMB has also been identified as osteoactivin in osteoblasts<sup>19</sup>, as well as being isolated from dendritic cells such as DC-HIL, a dendritic cell-associated transmembrane protein that promotes RGD (Arg-Gly-Asp)-dependent adhesion of endothelial cells through recognition of heparan sulfate proteoglycans<sup>20</sup>. In addition, it was reported that Gpnmb expressed on antigen-presenting cells negatively regulates T-cell activation by binding to syndecan 4, which is also expressed on these cells<sup>21,22</sup>. Indeed, we noted that—in addition to eliminating Gpnmb-positive (Gpnmb<sup>high</sup>) senescent cells—Gpnmb vaccination likely eliminated senescent cells expressing lower levels of Gpnmb (Fig. 3e and Extended Data Figs. 2i and 3d,e). Thus, further investigations

are required to elucidate how Gpnmb vaccination could affect the immune system and improve pathological aging.

#### Methods

Human samples. The ethical committee of Niigata University reviewed and approved the protocol of the human study on GPNMB expression and written informed consent was obtained from all subjects before enrollment. We enrolled 70 subjects admitted to Niigata University Medical and Dental Hospital. RNA samples prepared from leukocytes by using RNA extraction kits according to the manufacturer's instructions were subjected to quantitative polymerase chain reaction (qPCR) analysis. For immunohistochemical examination of GPNMB expression, arteries were obtained from patients who underwent cardiovascular surgery at Niigata University Medical and Dental Hospital. Paraffin-embedded sections (5  $\mu$ m) were prepared and stained with anti-GPNMB antibody (1:100, ab175427, Abcam) for 1 h at 37 °C. Then the sections were incubated with a goat antimouse IgG H + L (Cy5) secondary antibody (1:100 ab6563, Abcam) for staining GPNMB, with biotin-XX isolectin GS-IB4 conjugate (1:100, I21414, Invitrogen) for staining endothelial cells, and with Hoechst (1:1,000, 33258, Invitrogen) for labeling nuclei.

Animal models. All of the animal experiments were conducted in compliance with protocols reviewed by the Institutional Animal Care and Use Committee of Niigata University and approved by both the committee and the President of Niigata University. C57BL/6 mice were purchased from SLC Japan (Shizuoka), and were maintained on a HFD (CLEA) or normal chow (NC) from 4 to 12 weeks of age, unless otherwise described in the figure legends. In some experiments, C57BL/6 mice were fed a HFD from 4 weeks of age and were treated with senolytics or vehicle by oral gavage at 8 and 12 weeks of age for five consecutive days followed by analysis at 16 and 24 weeks. The DBA/2J and DBA/2J-Gpnmb+ mice were obtained from the Jackson Laboratory. DBA2J mice have a Gpnmb stop codon mutation (R150X)23 and were used to generate the Gpnmb KO model. Male DBA/2 I mice were mated with C57BL/6 mice to obtain Gpnmb+/- mice, and then were backcrossed with C57BL/6 mice for more than six generations. DBA/2J-Gpnmb+ mice with a C57BL/6 background were used as the control. Genotyping of Gpnmb-/- mice was performed as described previously<sup>24</sup>. To obtain Gpnmb-DTR-luciferase mice, the BAC clone (RP23-284O3, ~200 kb) containing the complete 21.7-kb mouse Gpnmb gene sequence with an additional 97 kb of the 5'-flanking region and 80 kb of the 3'-flanking region was purchased from Advanced Geno Techs Co. A chimeric Gpnmb-DTR-2A-luciferase BAC transgenic construct containing a tandem cassette of the human heparin-binding epidermal growth factor-like growth factor together with the DTR-generating I117V/L148V mutation, the 2A peptide gene, and a luciferase reporter gene was generated by recombineering. The DTR-2A-luciferase gene was transferred to the Gpnmb BAC clone by using the Red/ET Counter Selection BAC Modification Kit (Gene Bridges). Gpnmb-DTR-luciferase mice were obtained by pronuclear injection in C57BL/6 mouse embryos. Transgenic founders of the BAC transgenic construct were assessed by Southern blotting of Hinc I-digested tail DNA and probing with the [32P] labeled luciferase gene fragment. We obtained 20 founder lines of Gpnmb-DTRluciferase mice, and selected two lines with high copy numbers (~10 copies: lines 2-2 and 5-4). We confirmed that two independent mouse lines had similar phenotypes. To create a model of dietary obesity, Gpnmb-DTR-luciferase mice were maintained on the HFD from 4 to 16 weeks of age, unless otherwise described in the figure legends. For DT treatment, mice were intraperitoneally injected with DT (50 µg kg-1 body weight) twice at a 2-week interval (at 12 weeks and 14 weeks of age) and were analyzed at 16 weeks of age, unless otherwise described in the figure legends. ApoE KO mice (C57BL/6 background) were obtained from the Jackson Laboratory and were maintained on a second HFD (Oriental Yeast Co., Ltd.) from 4 to 16 weeks of age. ApoE KO/Gpnmb-DTRluciferase mice (C57BL/6 background) were obtained by crossing ApoE KO mice with Gpnmb-DTR-luciferase mice. ApoE KO/Gpnmb-DTR-luciferase mice were fed the second HFD from 4 weeks, treated with DT at 12 weeks and 14 weeks, and analyzed at 16 weeks of age. We utilized Zmpste24 KO mice (a model of Hutchinson-Gilford progeria syndrome) as a mouse model of premature aging. Generation and genotyping of Zmpste24 KO mice (MGI: 2158363) were done as described previously (http://www.informatics.jax.org/allele/MGI:2158363). p19ARF-DTR-luciferase mice (C57BL/6 background) were also generated and genotyped as described previously14.

Histological examination. SA-beta-gal activity was examined in adipose tissue as described previously<sup>8</sup>. Atherosclerotic plaque was estimated by assessing sections with Oil Red O staining. Briefly, whole aortas were dissected to remove adventitial fat, opened, and pinned flat for fixing in 4% paraformaldehyde for 12 h at room temperature. Then the pinned aortas were washed for 1 min with 60% isopropyl alcohol and incubated in 0.5% Oil Red O solution (Sigma-Aldrich) in 60% isopropyl alcohol) for 15 min at 37 °C for staining. Subsequently, the samples were briefly immersed in 60% isopropyl alcohol solution and then washed with double distilled water. After the Oil Red O-stained specimens were photographed, quantification of the plaque area was done with ImageJ.

**Physiological analyses.** Mice were housed individually to monitor their health status. Open field testing was performed in a  $50 \times 50 \, \text{cm}^2$  box, and total movements and average speed were analyzed with Time OFCR1 (O'Hara & Co., Ltd.) according to the manufacturer's instructions.

In vivo luciferase imaging analysis. In vivo luciferase imaging analysis was performed with an in vivo imaging system (IVIS; Perkin Elmer). Mice were shaved on the ventral surface, anesthetized with isoflurane (Wako Pure Chemicals Industries), and injected intraperitoneally with luciferin (150 mg kg<sup>-1</sup> body weight) according to the manufacturer's instructions (Vivo-Glo; Promega). Luciferase activity was monitored from 5 min after the luciferin injection, and signals were analyzed by using Living Image software (Perkin Elmer) to quantify luciferase activity.

Assessment of systemic metabolic parameters. Mice were housed individually for 1 week before performing the experiments. On the day of the GTT, mice were fasted for 6 h and then glucose was injected intraperitoneally at a dose of  $1\,\mathrm{g\,kg^{-1}}$  (body weight) in the early afternoon. For the ITT, mice were given human insulin intraperitoneally ( $1\,\mathrm{U\,kg^{-1}}$  body weight). Blood was collected from the tail vein at 0, 15, 30, 60 and 120 min after administration of each agent and blood glucose levels were measured with a glucose analyzer (Sanwa Kagaku Kenkyusho). Oxygen consumption was measured by an  $O_2/CO_2$  metabolic measurement system (Model MK-5000, Muromachi Kikai) as previously described 25.

Vaccination. A KLH-conjugated antigenic peptide (20 µg) and an equal volume of Titer Max Gold (Titer Max USA, Inc.) were emulsified according to the manufacturer's instructions. Two peptide sequences (A: RRGDGRWKD and B: RSQHLRFPDR) from the extracellular domain of Gpnmb were selected to create vaccines. Mice were fed the HFD (CLEA) or NC from 4 weeks of age, a KLHconjugated peptide with Titer Max Gold was injected subcutaneously at 8 weeks of age for immunization, and analysis was performed at 16 weeks. In the same manner, ApoE KO mice, Gpnmb KO mice, and their littermate controls were fed the HFD from 4 weeks of age, a KLH-conjugated peptide with Titer Max Gold was injected subcutaneously at 8 weeks of age for immunization, and analysis was done at 16 weeks. Aged mice fed NC were vaccinated at 50 weeks of age. The open field test was performed before and after vaccination (70 weeks of age). Zmpste24 mice fed NC were vaccinated at 10 weeks of age. p19Arf-DTR-luciferase mice were fed the HFD from 8 weeks of age, vaccinated at 13 weeks and analyzed at 21 weeks. In all experiments, the control group received an equal volume of KLH mixed with Titer Max Gold. A blood sample was collected from the tail vein of each mouse and plasma was obtained to measure antibody titers to each peptide by enzyme-linked immunosorbent assay. A 96-well microtiter plate (Nunc-Immuno MicroWell 96well solid plate; Thermo Scientific) was coated with one of the antigenic peptides conjugated to bovine serum albumin in carbonate buffer. After coating, plasma from immunized mice was added to the wells and incubated overnight. Then the plate was incubated with the secondary antibody (ECL antimouse IgG, horseradish peroxidase linked whole sheep antibody; GE Healthcare). After reaction with the TMB substrate (T0440; Sigma-Aldrich), the optical density was measured at  $450\,\mathrm{nm}$  (OD  $_{450}$  ) using an iMark microplate reader (Bio-Rad). The antibody titer against Gpnmb was higher with the vaccine containing peptide A, so this was used for all experiments reported here, although we found a modest effect of the vaccine containing peptide B on HFD-induced metabolic dysfunction. In some vaccination experiments, a neutralizing antibody was injected intraperitonially once a week from 9 weeks of age (that is, from one week after immunization). The neutralizing antibodies used were antimouse NK1.1 (200  $\mu g$  per body, 108760, Biolegend) and antimouse CD8β (Lyt 3.2) (200 µg per body, BE0223, BioXcel).

FACS analysis. To isolate the SVF from gWAT, fat was excised, minced and digested with digesting solution (0.5  $\mathrm{U\,ml^{-1}}$  collagenase type II (Worthington), 0.8 U ml<sup>-1</sup> dispase (Gibco) and 1 mM calcium chloride (CaCl<sub>2</sub>) in phosphatebuffered saline (PBS)) for 20 min at 37 °C. To isolate cells from the aorta, the aorta was excised, minced and digested with digesting solution (1.5  $\mathrm{U}\,\mathrm{ml^{-1}}$  collagenase type II, 2.4 U ml<sup>-1</sup> dispase and 1 mM CaCl<sub>2</sub> in PBS) for 20 min at 37 °C. The tissue lysate was subsequently filtered through a nylon mesh ( $40\,\mu m$ ), and red blood cell lysis was achieved with an ammonium chloride-based lysing buffer (Pharm Lyse, 555899, BD). Cells were resuspended in PBS supplemented with 1% fetal bovine serum (FBS) and 5 mM ethylenediammine tetraacetic acid (EDTA), incubated with Fc $\gamma$  blocker (1  $\mu g$  per million cells in 100  $\mu l$ , 553141, BD) at 4  $^{\circ}$ C for 5 min and stained with the following antibodies and  $10\,\mu\text{M}$  SPiDER-beta-Gal (Do-Jindo, SG02) for 30 min on ice: BV421-conjugated antimouse CD31 (1:100, 102408, BioLegend), PE/Cy7-conjugated antimouse CD45 (1:100, 103114, BioLegend), BB700-conjugated antimouse Cd11b (1:100, 564454, BD), PE/Cy7-conjugated antimouse CD3e (1:100, 100308, BioLegend), BV510-conjugated antimouse CD3 (1:100, 100234, BioLegend), APC/Cy7-conjugated antimouse Nk1.1 (1:100, 108724, BioLegend), APC/Fire750-conjugated antimouse Nk1.1 (1:100, 108752, BioLegend), BV650-conjugated antimouse F4/80 (1:100, 123149, BioLegend), Pacific Blue-conjugated antimouse Ly6G (1:100, 127611, BioLegend), BV510conjugated antimouse CD14 (1:100, 100234, BioLegend), BV785-conjugated antimouse CD14 (1:100, 123337, BioLegend), eFluor660-conjugated antimouse

Gpnmb (1:100, 50-5708-82, eBioscience) and eFluor660-conjugated antimouse IgG2ak Isotype control (1:100, 50-4321-82, eBioscience). Cells were then washed and resuspended in FACS buffer and analyzed by a spectral cell analyzer (ID7000, Sony). Data were collected and analyzed with ID7000 software (Sony, v.1.1.0.11041). The gating strategies are shown in the Supplementary Data.

**Cell culture.** HUVECs were purchased from Lonza and cultured according to the manufacturer's instructions. Senescent cells were identified as the cells in cultures that did not show an increase of cell numbers and remained subconfluent for 2 weeks. We confirmed that these cells were senescent by performing the SA-beta-gal activity assay. Mouse preadipocytes were isolated and cultured as described. According to the manufactured as described.

Isolation of endothelial cells. Lungs were harvested from mice for isolation of endothelial cells as described previously  $^{27}$ . Tissues were minced into small pieces with dissecting scissors and then incubated with digesting solution (0.5 U ml $^{-1}$  collagenase type II (Worthington), 0.8 U ml $^{-1}$  dispase (Gibco) and 1 mM CaCl $_2$  in PBS) for 45 min at 37 °C. Every 15 min, the samples were pipetted to fracture cell clumps and achieve dissociation into single cells. Tissue digestion was stopped by adding Dulbecco's modified eagle's medium (DMEM) containing 20% FBS. To remove connective tissue and fibers, the digested samples were passed through cotton gauze and nylon cell strainers (70 µm and 40 µm, BD Falcon). Then the samples were centrifuged at 300g for 5 min and resuspended in MACS buffer (PBS containing 1% FBS and 2 mmoll $^{-1}$  EDTA). CD45 $^{+}$  cells were removed from the harvested cells by the magnetic-activated cell sorting (MACS) technique with rat antimouse CD45 (BD550539, BD) and Dinabeads sheep antiRat IgG (11035, Invtrogen), after which CD31 $^{+}$  cells were selected with rat antimouse CD31 (BD553369, BD) and Dinabeads sheep antiRat IgG (11035, Invtrogen).

RNA analysis. Total RNA (1  $\mu$ g) was isolated from tissue samples with RNA-Bee (TEL-TEST Inc.) Real-time quantitative PCR (qPCR) was performed by using a Light Cycler 480 (Roche) with the Universal Probe Library and Light Cycler 480 Probes Master (Roche) according to the manufacturer's directions. The primers used and their sequences were as follows (*Rplp0*, *RPLP0* or *ACTB* was used as the internal control).

Mouse primers:

Gpnmb; 5'-ACGGCAGGTGGAAGGACT-3', 5'-CGGTGAGTCACTGGTC AGG-3'

Cdkn1a; 5'-TCCACAGCGATATCCAGACA-3', 5'-GGACATCACCAGGAT TGGAC-3'

 $\label{eq:cdkn2a} \textit{Cdkn2a}; 5'\text{-}\text{GGGTTTTCTTGGTGAAGTTCG-3}', 5'\text{-}\text{TTGCCCATCATCATCATCACCT-3}'$ 

 $\textit{Rplp0}; 5'\text{-}ACAATGCCCAGGGAAGACAG-3', 5'\text{-}ACAATGAAGCATTTTGGATAA-3'}$ 

Human primers:

*GPNMB*; 5'-ACCCACCCCTTCTTTAGGAC-3', 5'-TCTGGCAGTTTTCA TCAGGA-3'

 $CDKN1A; 5'\text{-}TCACTGTCTTGTACCCTTGTGC-3', 5'\text{-}GGCGTTTGGAGTGGTAGAAA-3'}$ 

CDKN2A; 5'-GTGGACCTGGCTGAGGAG-3', 5'-CTTTCAATCGGGGATGTCTG-3'

RPLP0; 5'-TCTACAACCCTGAAGTGCTTGAT-3', 5'-CAATCTGCAGACA GACACTGG-3'

 $ACTB; 5'\text{-}CCAACCGCGAGAAGATGA-3'}, 5'\text{-}CCAGAGGCGTACAGGGATAG-3'}$ 

RNA sequencing analysis. Total RNA was extracted from young and senescent HUVECs or aorta samples obtained from ApoE KO mice treated with Gpnmb or control vaccination using the RNeasy Plus Micro Kit (Qiagen). The complemenary DNA libraries were generated using the NEBNext Ultra RNA Library Prep Kit (New England BioLabs). The quality of total RNA and cDNA were assessed using the Agilent 2100 Bioanalyzer with the RNA6000 nano Kit and the DNA7500 kit (Agilent Technologies). Sequencing was performed using the HiSeq1500 system (Illumina) with a single-read sequencing length of 60 bp. A quality check of the sequencing data was performed by FaQCs (v.1.34). The TopHat analysis (v.2.0.13) was used to map the reference genome (GRCh38/hg38), with annotation data downloaded using the Ensembl Asia website (URL https://asia.ensembl.org/). Expression of each transcript was quantified as the number of fragments per kilobase of transcript per million fragments mapped. Expression of each transcript was compared between the two groups (young and senescent HUVECs or Gpnmb and control vaccine) via the Cuffdiff program (v.2.2.1). Gene expression data obtained in these studies were deposited in the Gene Expression Omnibus database (GSE155680 for HUVECs and GSE155596 for ApoE KO mice).

Western blot analysis. Whole-cell lysates were prepared in lysis buffer (10 mmol l<sup>-1</sup> Tris-HCl, pH 8, 140 mmol l<sup>-1</sup> sodium chloride, 5 mmol l<sup>-1</sup> EDTA, 0.025% sodium azide, 1% Triton X-100, 1% deoxycholate, 0.1% sodium dodecyl sulfate (SDS), 1 mmol l<sup>-1</sup> phenyl-methylsulphonyl fluoride, 5  $\mu g$  ml<sup>-1</sup> leupeptin, 2  $\mu g$  ml<sup>-1</sup> aprotinin, 50 mmol l<sup>-1</sup> sodium fluoride, and 1 mmol l<sup>-1</sup> sodium orthovanadate). Then lysates (40–50  $\mu g$ ) were resolved by SDS–polyacrylamide gel electrophoresis and proteins

were transferred to PVDF membranes (Millipore), which were incubated with the primary antibody followed by incubation with horseradish peroxidase-conjugated antirabbit or antimouse immunoglobulin-G (Jackson). Specific proteins were detected by enhanced chemiluminescence (Amersham). The primary antibodies for western blotting were anti-p53 antibody (2524; Cell Signaling), anti-p21 antibody (ab7960; Abcam), anti-Gpnmb antibody (AF2330; R&D Systems), antiactin antibody (4967; Cell Signaling) and anti-glyceraldehyde-3-phosphate dehydrogenase (GAPDH) antibody (sc-20357; Santa Cruz). For studies of human vascular endothelial cells, anti-p53 antibody (DO1) (sc-126; Santa Cruz), anti-p21 antibody (OP64-20UG; Calbiochem), anti-p16 antibody (554079; BD) and anti-GPNMB antibody (13251; Cell Signaling) were used. All primary antibodies were employed at a dilution of 1:1000, except for antiactin antibody and anti-GAPDH antibody (1:5000). The secondary antibody for anti-p53 antibody (2524; Cell Signaling), anti-p21 antibody (OP64-20UG; Calbiochem) and anti-p16 antibody (554079; BD) was peroxidase-conjugated AffiniPure goat antimouse IgG (light chain specific) (115-035-174; Jackson ImmunoResearch). In addition, peroxidase-conjugated AffiniPure goat antimouse IgG (H+L) (115-035-003; Jackson ImmunoResearch) was the secondary antibody for anti-p53 antibody (DO1) (sc-126), while peroxidase-conjugated AffiniPure goat antirabbit IgG (H+L) (111-035-003; Jackson ImmunoResearch) was used for anti-GPNMB antibody (13251), antiactin antibody (4967) and anti-p21 antibody (ab7960), and peroxidase-conjugated AffiniPure donkey antigoat IgG (H+L) (705-035-147; Jackson ImmunoResearch) was employed for anti-GAPDH antibody (sc-20357) and anti-Gpnmb antibody. All secondary antibodies were added at a dilution of 1:10000. Full western blot images are shown in the Supplementary Data.

Bioinformatic analysis. Gene expression profiles for GSE37091 and GSE13712 were analyzed with the GEO2R analysis tool provided as a web service in the Gene Expression Omnibus database<sup>10</sup>. Genes showing threefold or greater upregulation in senescent samples in comparison with young samples were extracted. The presence or absence of transmembrane regions was predicted with TMHMM2.0 for protein sequences downloaded from the KEGG GENES database (2 May 2014 version)<sup>11,12</sup>, and this process identified ten genes with predicted transmembrane regions. From among them, we selected *GPNMB* as a candidate seno-antigen gene because there is evidence of a potential link between *GPNMB* and human aging<sup>13</sup>.

Assay of ADCC. ADCC was evaluated by using an mFc $\gamma$ RIV ADCC Reporter Bioassay, Core Kit (Promega). Target cells (replicative senescent preadipocytes from C57BL/6 mice) were added to 96-well plates at 10 $^{\circ}$  cells per well and were incubated for 30 min at 37 $^{\circ}$ C with purified IgG antibody from Gpnmb-vaccinated mice or KLH-vaccinated mice (control). After incubation, effector cells were added to the individual wells at an effector/target cell ratio of 1:1. Then the plates were incubated for a further 4h at 37 $^{\circ}$ C, and luminescence was measured with a plate reader (Nivo, Perkin Elmer).

Statistical analysis. Statistical analysis was done with SPSS software (version 24 or 25). All data were from different biological replicates and are shown as box and whisker plots that display the range of the data (whiskers), the 25th and 75th percentiles (box) and the median (solid line) or the mean ± SEM. Outliers and abnormal values were assessed by boxplot analysis. Differences between groups were examined by the two-tailed Student's *t*-test or one-way analysis of variance (ANOVA), followed by Tukey's multiple comparison test for comparisons among more than two groups. Line graphs (GTT, ITT and antibody titer and ADCC assay (mean ± SEM or SD)) with individual values were drawn by Graph Pad Prism (Prism8). Differences between groups were examined by repeated measures analysis followed by Tukey's multiple comparison test, or univariate analysis of variance was done for time course comparisons. Survival curves were drawn by the Kaplan–Meier method and compared with the log-rank test. In all analyses, P < 0.05 was considered to indicate statistical significance. The exact P values were also provided in source data.

**Reporting Summary.** Further information on research design is available in the Nature Research Reporting Summary linked to this paper.

#### Data availability

All data are available from the authors upon reasonable request. Additional materials, including the source data, are available online. RNAseq data and gene expression data obtained in these studies were deposited in the Gene Expression Omnibus database (GSE155680 for HUVECs and GSE155596 for ApoE KO mice).

Received: 26 August 2020; Accepted: 4 November 2021; Published online: 10 December 2021

#### References

- Baker, D. J. et al. Naturally occurring p16(Ink4a)-positive cells shorten healthy lifespan. *Nature* 530, 184–189 (2016).
- Xu, M. et al. Senolytics improve physical function and increase lifespan in old age. Nat. Med. 24, 1246–1256 (2018).

- Kirkland, J. L. & Tchkonia, T. Senolytic drugs: from discovery to translation. J. Intern. Med. 288, 518–536 (2020).
- Campisi, J. Senescent cells, tumor suppression, and organismal aging: good citizens, bad neighbors. Cell 120, 513–522 (2005).
- Childs, B. G. et al. Senescent cells: an emerging target for diseases of ageing. Nat. Rev. Drug Discov. 16, 718–735 (2017).
- Minamino, T. et al. Endothelial cell senescence in human atherosclerosis: role of telomere in endothelial dysfunction. Circulation 105, 1541–1544 (2002).
- Minamino, T. & Komuro, I. Vascular cell senescence: contribution to atherosclerosis. Circ. Res. 100, 15–26 (2007).
- 8. Minamino, T. et al. A crucial role for adipose tissue p53 in the regulation of insulin resistance. *Nat. Med.* **15**, 1082–1087 (2009).
- Shimizu, I., Yoshida, Y., Suda, M. & Minamino, T. DNA damage response and metabolic disease. Cell Metab. 20, 967–977 (2014).
- Barrett, T. et al. NCBI GEO: archive for functional genomics data sets-update. Nucleic Acids Res. 41, D991–D995 (2013).
- Kanehisa, M. et al. KEGG for linking genomes to life and the environment. Nucleic Acids Res. 36, D480–D484 (2008).
- Krogh, A., Larsson, B., von Heijne, G. & Sonnhammer, E. L. Predicting transmembrane protein topology with a hidden Markov model: application to complete genomes. *J. Mol. Biol.* 305, 567–580 (2001).
- Jiang, S. S. et al. Gene expression profiling suggests a pathological role of human bone marrow-derived mesenchymal stem cells in aging-related skeletal diseases. *Aging (Albany NY)* 3, 672–684 (2011).
- 14. Hashimoto, M. et al. Elimination of p19(ARF)-expressing cells enhances pulmonary function in mice. *JCI Insight* 1, e87732 (2016).
- Roos, C. M. et al. Chronic senolytic treatment alleviates established vasomotor dysfunction in aged or atherosclerotic mice. *Aging Cell* 15, 973–977 (2016).
- Palmer, A. K. et al. Targeting senescent cells alleviates obesity-induced metabolic dysfunction. Aging Cell 18, e12950 (2019).
- Aguayo-Mazzucato, C. et al. Acceleration of beta cell aging determines diabetes and senolysis improves disease outcomes. *Cell Metab.* 30, 129–142. e124 (2019).
- Weterman, M. A. et al. nmb, a novel gene, is expressed in low-metastatic human melanoma cell lines and xenografts. Int. J. Cancer 60, 73–81 (1995).
- Safadi, F. F. et al. Cloning and characterization of osteoactivin, a novel cDNA expressed in osteoblasts. J. Cell. Biochem. 84, 12–26 (2001).
- Shikano, S., Bonkobara, M., Zukas, P. K. & Ariizumi, K. Molecular cloning of a dendritic cell-associated transmembrane protein, DC-HIL, that promotes RGD-dependent adhesion of endothelial cells through recognition of heparan sulfate proteoglycans. J. Biol. Chem. 276, 8125–8134 (2001).
- Chung, J. S., Dougherty, I., Cruz, P. D. Jr. & Ariizumi, K. Syndecan-4 mediates the coinhibitory function of DC-HIL on T cell activation. *J Immunol* 179, 5778–5784 (2007).
- Chung, J. S., Sato, K., Dougherty, I. I., Cruz, P. D. Jr. & Ariizumi, K. DC-HIL is a negative regulator of T lymphocyte activation. *Blood* 109, 4320–4327 (2007).
- Anderson, M. G. et al. Mutations in genes encoding melanosomal proteins cause pigmentary glaucoma in DBA/2J mice. Nat. Genet. 30, 81–85 (2002).
- Katayama, A. et al. Beneficial impact of Gpnmb and its significance as a biomarker in nonalcoholic steatohepatitis. Sci. Rep. 5, 16920 (2015).
- Oike, Y. et al. Angiopoietin-related growth factor antagonizes obesity and insulin resistance. Nat. Med. 11, 400–408 (2005).
- Tchkonia, T. et al. Increased TNFalpha and CCAAT/enhancer-binding protein homologous protein with aging predispose preadipocytes to resist adipogenesis. Am. J. Physiol. Endocrinol. Metab. 293, E1810–E1819 (2007).
- Ieronimakis, N., Balasundaram, G. & Reyes, M. Direct isolation, culture and transplant of mouse skeletal muscle derived endothelial cells with angiogenic potential. *PLoS ONE* 3, e0001753 (2008).

#### Acknowledgements

This work was supported by a Grant-in-Aid for Scientific Research (A) (20H00533) from MEXT, AMED under grant number JP20ek0210114, and AMED-CREST under grant number JP20gm1110012, and Moonshot Research and Development Program (21zf0127003s0201), MEXT Supported Program for the Strategic Research Foundation at Private Universities Japan, Private University Research Branding Project, and Leading Initiative for Excellent Young Researchers, and grants from the Takeda Medical Research Foundation, the Vehicle Racing Commemorative Foundation, Ono Medical Research Foundation and the Suzuken Memorial Foundation (to T.M.). Support was also provided by a Grant-in-Aid for Scientific Research (C) from MEXT (18K08063) and a grant from the Suzuken Memorial Foundation, the SENSHIN Medical Research Foundation and the MSD Life Science Foundation (to M.S.). All funders had no role in study design, data collection and analysis, decision to publish or preparation of the manuscript.

#### **Author contributions**

T.M. contributed to establishment of the research concept and research design, wrote the manuscript and supervised all experiments. M. Suda wrote the manuscript, contributed

to designing the experiments and performed most of the experiments. I.S. contributed to designing the experiments, as well as the in vitro and in vivo studies. G.K. contributed to the in vitro and in vivo studies. Yohko Yoshida contributed to analyses of the genetic mouse models. Y.H. and R.I. assisted with the in vivo studies. A.K. and J.W. contributed to analysis of Gpnmb KO mice. M. Seki, Y.S. and A.I. contributed to epigenetic and transcriptome analyses. H.N. and R. Morishita contributed to experiments using the peptide vaccine. R. Mikawa and M. Sugimoto contributed to analysis of Gpnmb-DTR-luciferase mice and p19 $^{\rm ARF}$ -DTR-luciferase mice. A.N. and M.T. contributed to histological examination. S.O. contributed to bioinformatic analysis. K.O. contributed to analysis of human samples. Yutaka Yoshida, N.M. and M.N.M. contributed to analysis of lysosomes.

#### **Competing interests**

The authors declare no competing interests.

#### **Additional information**

Extended data is available for this paper at https://doi.org/10.1038/s43587-021-00151-2.

**Supplementary information** The online version contains supplementary material available at https://doi.org/10.1038/s43587-021-00151-2.

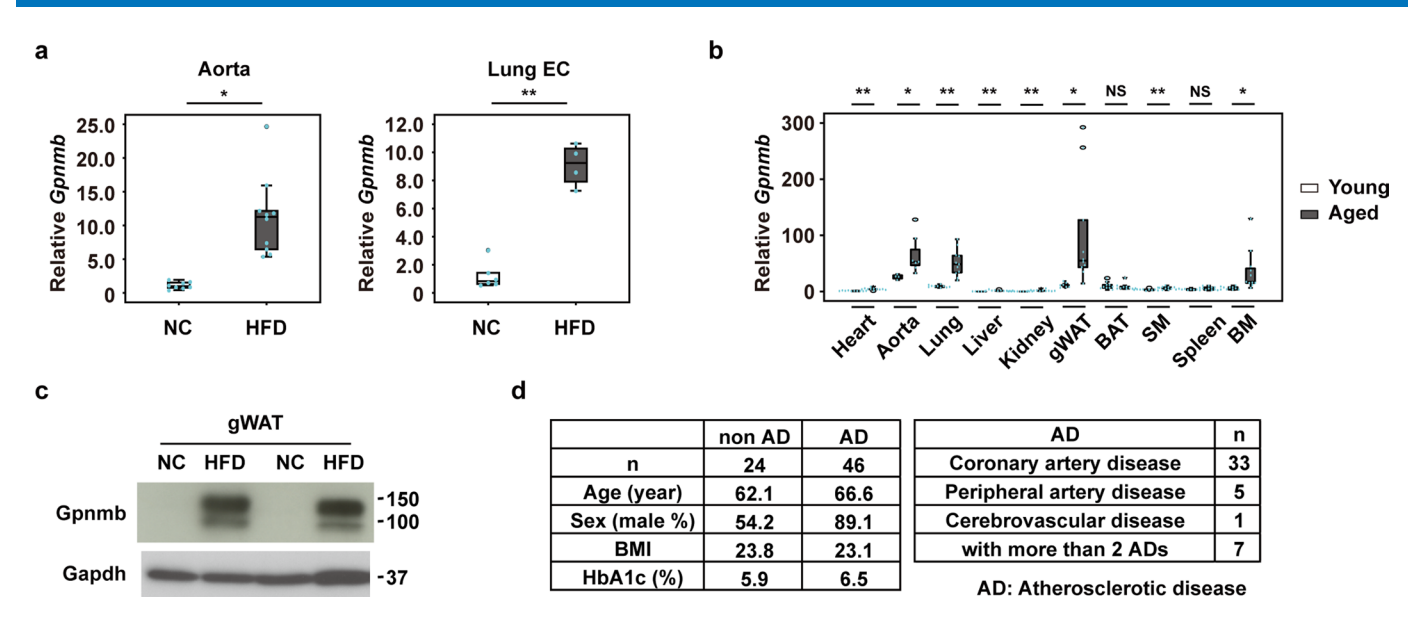
Correspondence and requests for materials should be addressed to Tohru Minamino.

**Peer review information** *Nature Aging* thanks Jeffrey Miller and the other, anonymous, reviewer(s) for their contribution to the peer review of this work.

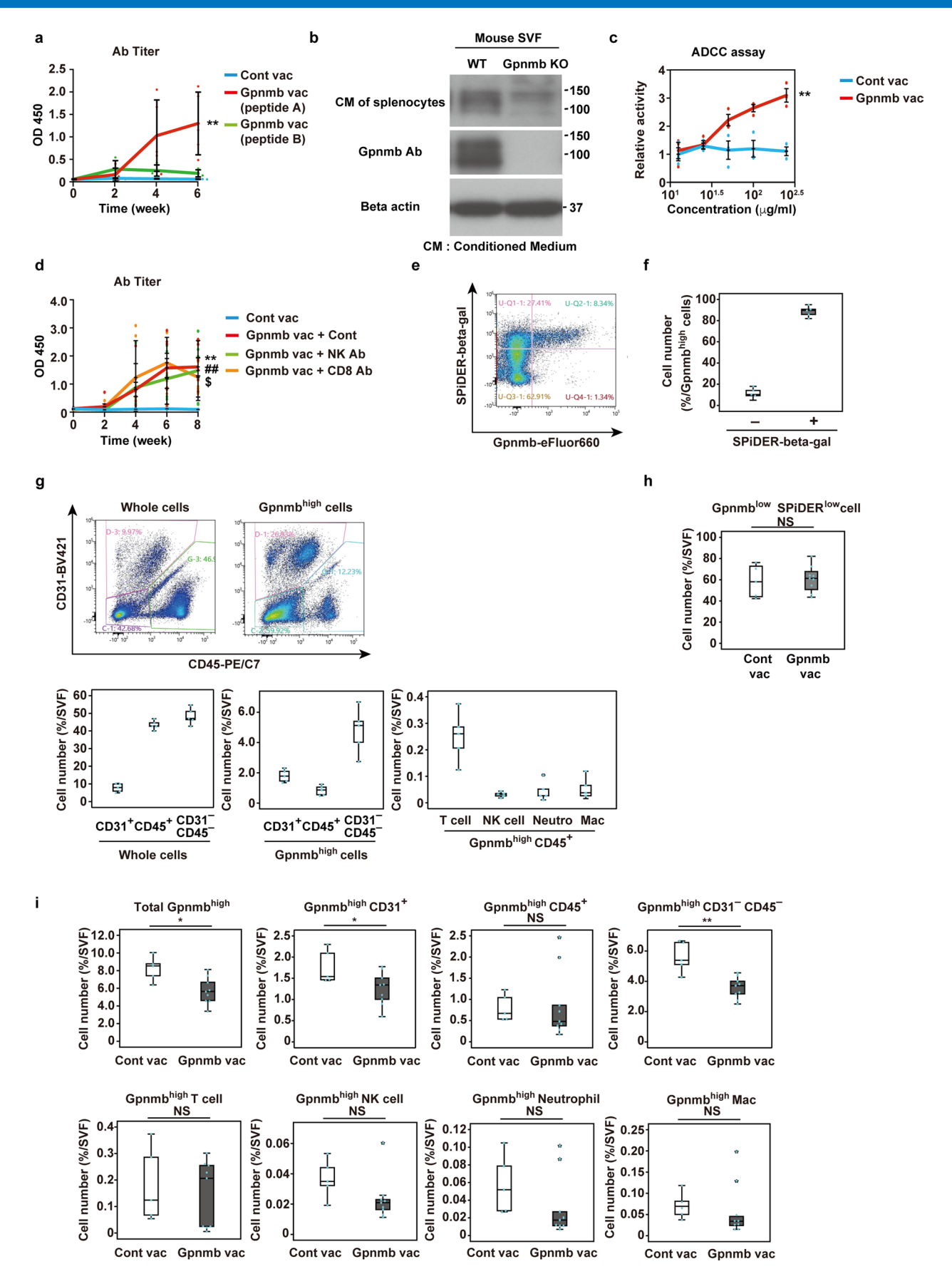
Reprints and permissions information is available at www.nature.com/reprints.

**Publisher's note** Springer Nature remains neutral with regard to jurisdictional claims in published maps and institutional affiliations.

© The Author(s), under exclusive licence to Springer Nature America, Inc. 2021

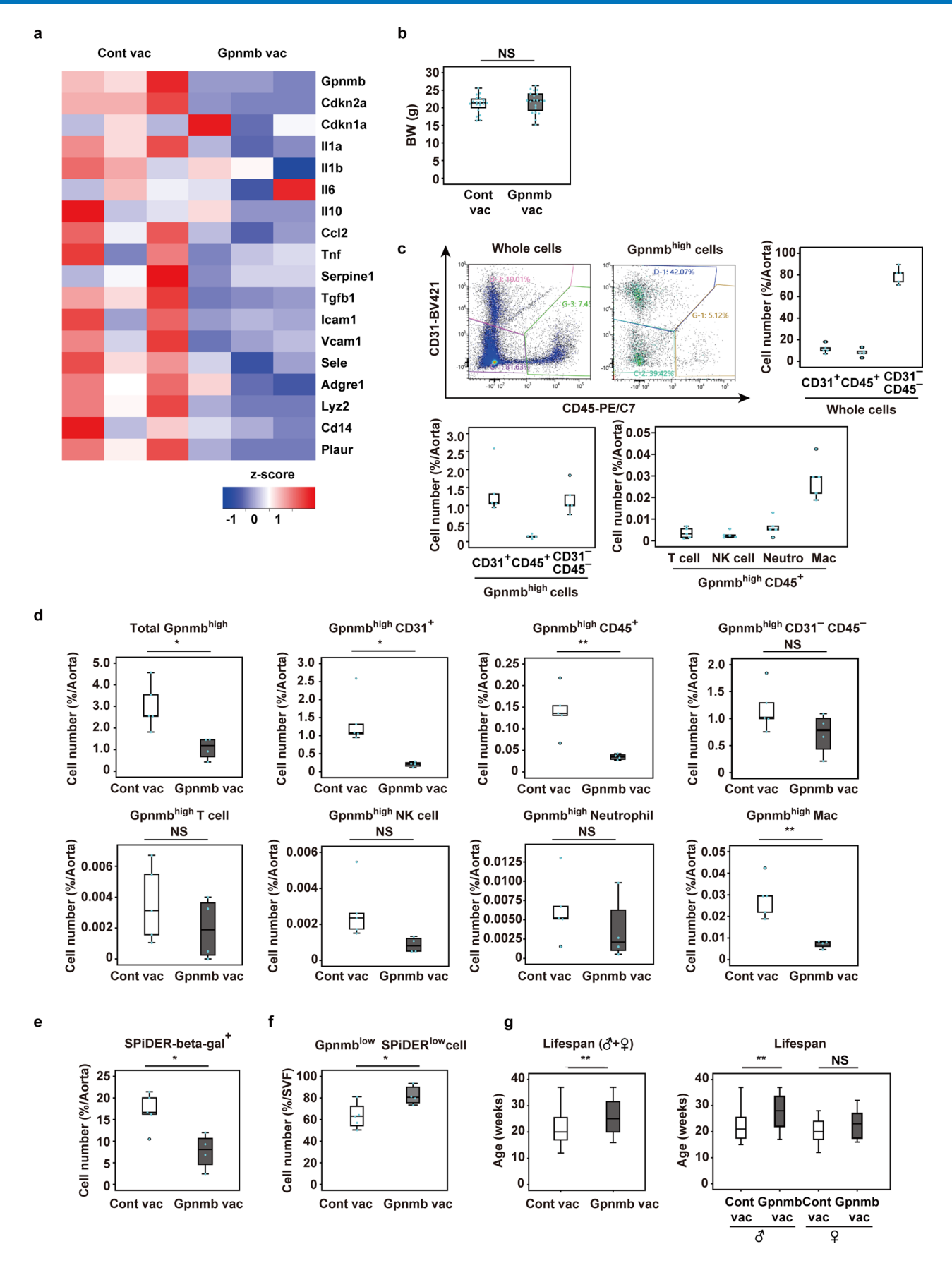


**Extended Data Fig. 1** [Expression of Gpnmb in various tissues. **a**, qPCR analysis of relative Gpnmb expression in the aorta or lung endothelial cells (EC) of mice fed NC or an HFD (aorta, n = 8 for NC and n = 10 for HFD; EC, n = 6 for NC and n = 4 for HFD). **b**, qPCR analysis of relative Gpnmb expression in various tissues of young mice (12 weeks old) and aged mice (109–110 weeks old) (heart, n = 10 for young mice and n = 11 for aged mice; lung, n = 10 for young mice and n = 11 for aged mice; liver, n = 5 for young mice and n = 10 for aged mice; kidney, n = 9 for young mice and n = 11 for aged mice; gWAT, n = 7 for young mice and n = 10 for aged mice; brown adipose tissue (BAT) n = 10 for both mice; skeletal muscle (SM), n = 10 for young mice and n = 9 for aged mice; spleen, n = 10 for young mice and n = 11 for aged mice). n = 10 for young mice and n = 11 for aged mice). n = 10 for young mice and n = 11 for aged mice). n = 10 for young mice and n = 11 for aged mice). n = 10 for young mice and n = 11 for aged mice). n = 10 for young mice and n = 11 for aged mice). n = 10 for young mice and n = 11 for aged mice). n = 10 for young mice and n = 11 for aged mice). n = 10 for young mice and n = 11 for aged mice). n = 10 for young mice and n = 11 for aged mice). n = 10 for young mice and n = 11 for aged mice). n = 10 for young mice and n = 11 for aged mice; bone marrow (BM), n = 10 for young mice and n = 11 for aged mice; bone marrow (BM), n = 10 for young mice and n = 11 for aged mice; bone marrow (BM), n = 10 for young mice and n = 11 for aged mice; bone marrow (BM), n = 10 for young mice and n = 11 for aged mice; bone marrow (BM), n = 10 for young mice and n = 11 for aged mice; bone marrow (BM), n = 10 for young mice and n = 11 for aged mice; bone marrow (BM), n = 10 for young mice and n = 11 for aged mice; bone marrow (BM), n = 10 for young mice and n = 11 for aged mice; bone marrow (BM), n = 10



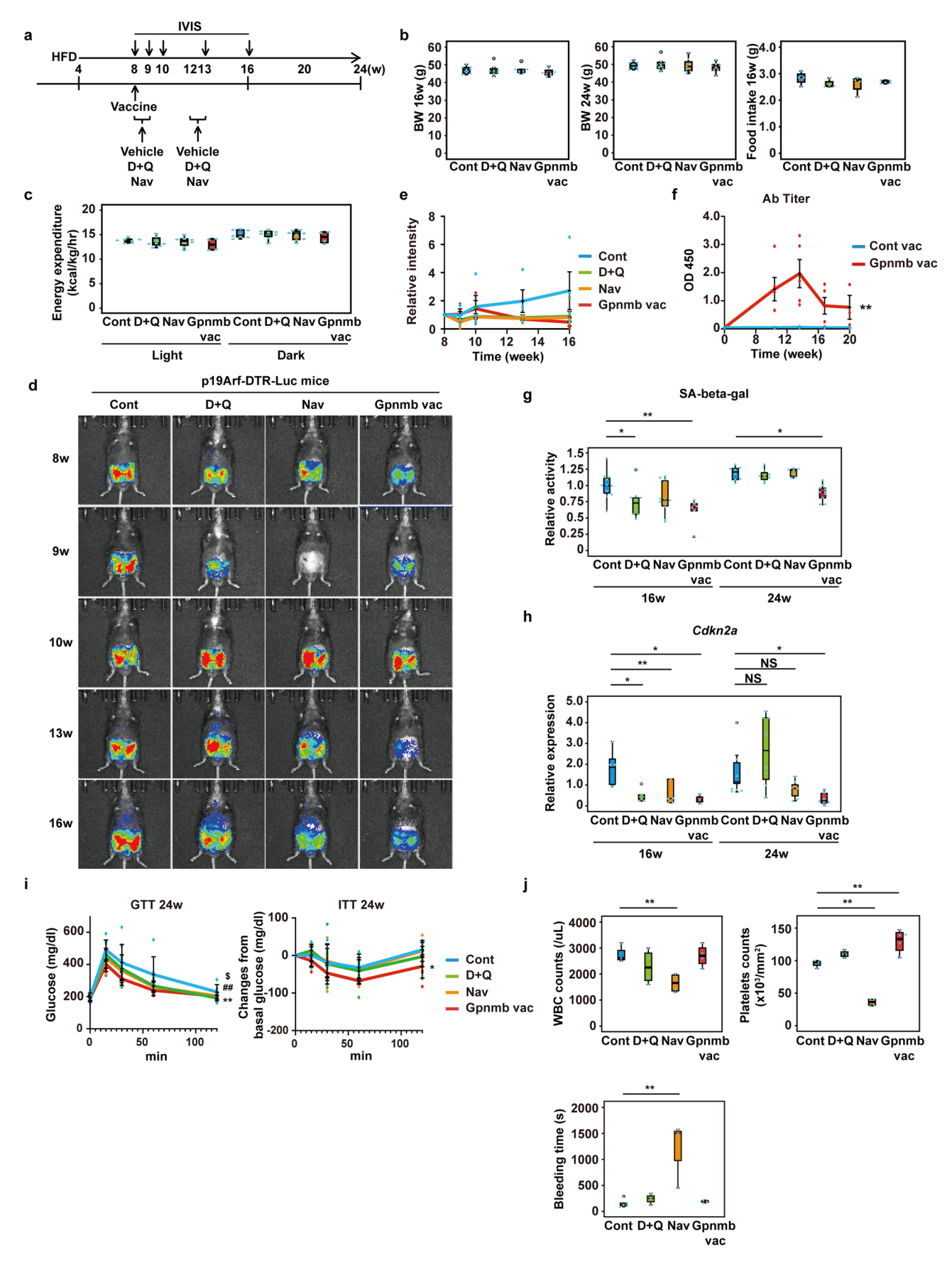
Extended Data Fig. 2 | See next page for caption.

Extended Data Fig. 2 | Gpnmb vaccination improves HFD-induced metabolic abnormalities.  $\bf{a}$ , Serum titer of anti-Gpnmb antibody (n = 5, 5, 4 for Cont, A, and B).  $\bf{b}$ , Western blot analysis of Gpnmb expression in senescent cells of the stromal vascular fraction (SVF) from wild-type mice (WT) and Gpnmb knockout (KO) mice. The similar results were obtained from three independent experiments.  $\bf{c}$ , ADCC activity of purified IgG antibody from mice immunized with Gpnmb vaccine (Gpnmb vac) or control vaccine (Cont vac) (n = 3 each).  $\bf{d}$ , Serum titer of anti-Gpnmb antibody in mice administered Gpnmb vaccine plus a neutralizing antibody (n = 8, 8, 6, and 6 for Cont vac, Gpnmb vac+Cont, Gpnmb vac+NK, and Gpnmb vac+CD8, respectively).  $\bf{e}$ , FACS analysis for SPiDER-beta-gal and Gpnmb expression in the SVF of HFD-fed mice.  $\bf{f}$ , The number of SPiDER-beta-gal-positive cells among Gpnmb<sup>high</sup> cells in the SVF (n = 5).  $\bf{g}$ , Cellular populations expressing Gpnmb in the SVF from visceral adipose tissue (n = 5).  $\bf{h}$ , The number of Gpnmb<sup>low</sup> SPiDER-beta-gal<sup>low</sup> cells in the SVF (Cont vac, n = 5; Gpnmb vac, n = 9).  $\bf{i}$ , FACS analyses of the SVF from HFD-fed mice (Cont vac, n = 5; Gpnmb vac, n = 9). The data were analyzed by the 2-tailed Student's t-test ( $\bf{h}$  and  $\bf{i}$ ) or repeated measures analysis followed by Tukey's multiple comparison test ( $\bf{a}$ ,  $\bf{c}$ , and  $\bf{d}$ ). \*P < 0.05; \*P < 0.01; NS, not significant. In Extended Data Fig. 2a, \*\*P < 0.01 Cont vac vs. Gpnmb vac (peptide A). In Extended Data Fig. 2d, ##P = 0.026 Cont vac vs. Gpnmb + NK, \*P = 0.005 Cont vac vs. Gpnmb vac + CD8, \*\*P = 0.004 Cont vac vs. Gpnmb vac + Cont. The data are shown as box and whisker plots that display the range of the data (whiskers), the 25th and 75th percentiles (box), and the median (solid line) ( $\bf{f}$ - $\bf{i}$ ), the mean  $\pm$  SEM with plots of all individual data ( $\bf{a}$  and  $\bf{d}$ ), or the mean  $\pm$  SD with plots of all individual data ( $\bf{c}$ ).



Extended Data Fig. 3 | See next page for caption.

**Extended Data Fig. 3 | Gpnmb vaccination improves phenotypes of pathological aging. a**, Aortic samples obtained from ApoE KO mice treated with Gpnmb or control vaccine were subjected to RNA sequencing analysis (n=3, respectively). **b**, Body weight (BW) of ApoE KO mice (Cont vac, n=19; Gpnmb vac, n=20). **c**, Cell populations expressing Gpnmb in the aorta from ApoE KO mice (n=5). Outlier values were detected by boxplot analysis and was excluded from statistical assessment as indicated in Source data. **d**, FACS analyses of the aorta of ApoE KO HFD-fed mice treated with Gpnmb vaccine (Gpnmb vac) or control vaccine (Cont vac) (n=5 for Cont vac and n=4 for Gpnmb vac). **e**, FACS analysis with SPiDER-beta-gal of the aorta from ApoE KO mice treated with Gpnmb vaccine (Gpnmb vac) or control vaccine (Cont vac) (n=5 for Cont vac and n=4 for Gpnmb vac). **f**, The number of Gpnmblow SPiDER-beta-gallow cells in the aorta of ApoE KO HFD-fed mice (Cont vac, n=5; Gpnmb vac, n=4). **g**, Lifespan of Zmpste24 KO mice treated with Gpnmb vaccine (Gpnmb vac) or control vaccine (Cont vac) at 10 weeks of age (Cont vac, n=19 for male mice and n=18 for female mice; Gpnmb vac, n=19 for male mice and n=16 for female mice). The data were analyzed by the 2-tailed Student's t-test (**b**, **d**, **e**, **f**, and **g**). \*P < 0.05; \*\*P < 0.01; NS, not significant. The data are shown as box and whisker plots that display the range of the data (whiskers), the 25th and 75th percentiles (box), and the median (solid line) (**b-g**).



Extended Data Fig. 4 | See next page for caption.

**Extended Data Fig. 4 | Treatment with senolytics and dietary metabolic abnormalities. a**, Experimental protocol. **b**, Body weight (BW) and food intake of mice treated with vehicle (Cont), dasatinib and quercetin (D+Q), Navitoclax (Nav), or Gpnmb vaccine (Gpnmb vac) (body weight n=8, 8, 7, 8, food intake 4, 4, 4, 5). **c**, Energy expenditure (n=7, 8, 8, 4). **d**, Luciferase activity. **e**, Relative luciferase activity (n=3, 5, 5, and 3). **f**, Serum titer of anti-Gpnmb antibody. (n=5, 5 for 0, 8, 12, 16 weeks, n=3, 3 for 20 weeks). **g**, Assay of SA-beta-gal (n=11, 10, 12 and 6 for 16 weeks, and n=8, 8, 7 and 10 for 24 weeks). **h**, Relative expression of *Cdkn2a* (n=4, 5, 5, and 3 for 16 weeks and n=7, 8, 7, and 7 for 24 weeks). **i**, Glucose tolerance test (GTT, left) and insulin tolerance test (ITT, right) (n=6, 8, 7, and 7). Changes from basal glucose levels are shown in the ITT graph. **j**, White blood cell and platelet counts, and bleeding time (n=3, 4, 4, and 4 for white cell counts, n=3, 4, 4, and 4 for platelet counts, and n=5, 3, 3, and 3 for bleeding time). The data were analyzed by repeated measures analysis followed by Tukey's multiple comparison test (**b**, **c**, **g**, and **j**), by the 2-tailed Student's t-test (**h**), or by univariate analysis of variance or repeated measures analysis followed by Tukey's multiple comparison test (**f** and **i**). \*P < 0.05, \*\*P < 0.01, NS (not significant). In Extended Data Fig. 4i, \*P = 0.024, \*\*P < 0.001 Cont vs. Gpnmb vac, \*P = 0.018 Cont vs. D + Q, \*\*P = 0.007 Cont vs. Nav. The data are shown as box and whisker plots that display the range of the data (whiskers), the 25th and 75th percentiles (box), and the median (solid line) (**b**, **c**, **g**, **h**, and **j**) or the mean  $\pm$  SEM with plots of all individual data (**h** and **j**).

### nature portfolio

Corresponding author(s):	Tohru Minamino
Last updated by author(s):	Oct 27, 2021

#### **Reporting Summary**

Nature Portfolio wishes to improve the reproducibility of the work that we publish. This form provides structure for consistency and transparency in reporting. For further information on Nature Portfolio policies, see our <u>Editorial Policies</u> and the <u>Editorial Policy Checklist</u>.

~					
St	۲a	ıΤı	IC.	ŀι	$\sim$

For a	all statistical analyses, confirm that the following items are present in the figure legend, table legend, main text, or Methods section.
n/a	Confirmed
	igwedge The exact sample size ( $n$ ) for each experimental group/condition, given as a discrete number and unit of measurement
	🔀 A statement on whether measurements were taken from distinct samples or whether the same sample was measured repeatedly
	The statistical test(s) used AND whether they are one- or two-sided  Only common tests should be described solely by name; describe more complex techniques in the Methods section.
$\boxtimes$	A description of all covariates tested
$\boxtimes$	A description of any assumptions or corrections, such as tests of normality and adjustment for multiple comparisons
	A full description of the statistical parameters including central tendency (e.g. means) or other basic estimates (e.g. regression coefficient AND variation (e.g. standard deviation) or associated estimates of uncertainty (e.g. confidence intervals)
	For null hypothesis testing, the test statistic (e.g. <i>F</i> , <i>t</i> , <i>r</i> ) with confidence intervals, effect sizes, degrees of freedom and <i>P</i> value noted <i>Give P values as exact values whenever suitable.</i>
$\boxtimes$	For Bayesian analysis, information on the choice of priors and Markov chain Monte Carlo settings
$\boxtimes$	For hierarchical and complex designs, identification of the appropriate level for tests and full reporting of outcomes
$\boxtimes$	$\square$ Estimates of effect sizes (e.g. Cohen's $d$ , Pearson's $r$ ), indicating how they were calculated
	Our web collection on statistics for biologists contains articles on many of the points above.

#### Software and code

Policy information about availability of computer code

Data collection

Light cycler 480 (Roche version 1.5.1), BZ-II viewer (Keyence v.2.1), BZ-II analyzer (Keyence v1.42), BZ-II analyzer (Keyence v1.42), Nivo (Perkin Elmer ver 3.0.2), Image J (version 10.2), Integrated genome viewer (version 2.50), ID 7000 (SONY version 1.1.0.11041), Living Image software (Perkin Elmer ver 4.5), Time OFCR1 (O'Hara & Co.,Ltd), O2/CO2 metabolic measurement system (Model MK-5000), Muromachi Kikai), FaQCs (version 1.34), TopHat analysis (version 2.0.13), Cuffdiff program (version 2.2.1), TrimGalore (v0.5.0), BWA (v0.7.17), MACS (v1.4.3), Picard (v2.18.20), TMHMM2.0 (the KEGG GENES database, May 2, 2014)

Data analysis

Data were analyzed with SPSS version 24 or 25 software.

For manuscripts utilizing custom algorithms or software that are central to the research but not yet described in published literature, software must be made available to editors and reviewers. We strongly encourage code deposition in a community repository (e.g. GitHub). See the Nature Portfolio guidelines for submitting code & software for further information.

#### Data

Policy information about <u>availability of data</u>

All manuscripts must include a data availability statement. This statement should provide the following information, where applicable:

- Accession codes, unique identifiers, or web links for publicly available datasets
- A description of any restrictions on data availability
- For clinical datasets or third party data, please ensure that the statement adheres to our policy

RNAseq data; Gene expression data obtained in these studies were deposited in the Gene Expression Omnibus database (GSE155680 for HUVECs and GSE155596 for ApoE KO mice).

<b>—</b> ·		ı		•			
FID.	$\Box$	l-sn	ecif	.I.C	$r \rho r$	ነ∩rt	าทธ
	u		CCII		$I \subset I$	$\mathcal{I}$	വാട്ട

i leiu-spe	ecine reporting
Please select the o	ne below that is the best fit for your research. If you are not sure, read the appropriate sections before making your selection.
\( \) Life sciences	Behavioural & social sciences Ecological, evolutionary & environmental sciences
For a reference copy of	the document with all sections, see <u>nature.com/documents/nr-reporting-summary-flat.pdf</u>
Life scier	nces study design
All studies must dis	sclose on these points even when the disclosure is negative.
Sample size	Sample sizes were determined based on previously published experiments where differences were observed (Aging mod; Nature. 2011 Nov 2;479(7372):232-6. Nat Med. 2018 Aug;24(8):1246-1256. Atherosclerotic assay; Science. 2016 Oct 28;354(6311):472-477. Metabolic assay; Nat Med. 2009 Sep;15(9):1082-7. Vascular assay; J Mol Cell Cardiol. 2019 Apr;129:105-117.) or were calculated by using mean and standard deviation from the preliminary experiments.
Data exclusions	All values were included for statistical analyses. Outliers were evaluated by boxplot analyses with SPSS version 24 or 25 software. Outliers in Figure 1h, 3d, and Extended data figure 3c were excluded from the analysis. Data exclusions are clearly described in each figure legend, in Excel format source data files.
Replication	All data were from different biological replicates as indicated in each figure legend and all findings were reliably reproduced in several independent cohorts.
Randomization	All mice were randomly allocated for treatments and surgical procedures under blinded condition. For cell culture experiments, wells of cultured cells were sequentially assigned to distinct treatment groups.
Blinding	Investigators were blinded to mouse genotypes during experiments. All animal models were generated and analyzed under blinded condition.  Other experiments including in vitro study, investigators were blinded to allocation during experiments and outcome assessments.

#### Reporting for specific materials, systems and methods

We require information from authors about some types of materials, experimental systems and methods used in many studies. Here, indicate whether each material, system or method listed is relevant to your study. If you are not sure if a list item applies to your research, read the appropriate section before selecting a response.

Materials & experimental systems	Methods			
n/a Involved in the study	n/a Involved in the study			
Antibodies	ChIP-seq			
Eukaryotic cell lines	Flow cytometry			
Palaeontology and archaeology	MRI-based neuroimaging			
Animals and other organisms				
Human research participants				
Clinical data				
Dual use research of concern				
•				

#### **Antibodies**

Antibodies used

anti-human GPNMB antibody; used in western blotting, immunoprecipitation, Cell Signaling, #13251, [lot number 1]. anti-human GPNMB antibody; used in immunohistochemistry, Abcam, ab175427, [lot number GR256360-16]. anti-human p53 antibody; used in western blotting, Santa Cruz, sc-126, [lot number F2811]. anti-human p21 antibody; used in western blotting, Abcam, ab7960, [lot number GR175274-2]. anti-human p16 antibody; used in western blotting, BD, 554079, [lot number 17926]. anti-β actin antibody (13E5); used in western blotting, Cell Signaling, #4970, [lot number 9]. anti-mouse Gpnmb antibody; used in western blotting, R&D, AF2330, [lot number ULH0211101]. anti-mouse p53 antibody (1C12); used in western blotting, Cell Signaling, #2524, [lot number 13]. anti-mouse p21 antibody; used in western blotting, Carbiochem, OP64-20UG, [lot number D00141439]. anti-α-tubulin antibody (11H10); used in western blotting, Cell Signaling, #2125, [lot number 11]. anti-GAPDH antibody; used in western blotting, Santa Cruz, sc-20357, it has been discontinued. BV421-conjugated anti-mouse Cd31 antibody; used in flow cytometry, BioLegend, 102408, [B301862] PE/Cy7-conjugated anti-mouse Cd45 antibody; used in flow cytometry, BioLegend, 103114, [B308464] BB700-conjugated anti-mouse Cd11b antibody; used in flow cytometry, BD, 564454, [9093647] BV510-conjugated anti-mouse Cd3 antibody; used in flow cytometry, BioLegend, 100234, [B320432] BV605-conjugated anti-mouse Cd19 antibody; used in flow cytometry, BioLegend, 115539, [B324619] APC/Fire750-conjugated anti-mouse Nk 1.1 antibody; used in flow cytometry, BioLegend, 108752, [B326399]

```
BV650-conjugated anti-mouse F4/80 antibody; used in flow cytometry, BioLegend, 123149, [B309664] Pacific Blue-conjugated anti-mouse Ly-6G antibody; used in flow cytometry, BioLegend, 127611, [B288475] BV785-conjugated anti-mouse Cd14 antibody; used in flow cytometry, BioLegend, 123337, [B321510]
```

BV605-conjugated anti-mouse Cd11c antibody; used in flow cytometry, BioLegend, 117333, [B316089]

BV711-conjugated anti-mouse lcam1 (Cd54) antibody; used in flow cytometry, BioLegend, 116143, [B317417]

eFluor660-conjugated anti-mouse Gpnmb antibody; used in flow cytometry, eBioscience, 50-5708-82, [4314688]

eFluor660-conjugated anti-mouse IgG2ak Isotype control antibody; used in flow cytometry, eBioscience, 50-4321-82, [4331769] goat anti-mouse IgG H+L (Cy5) secondary antibody; used in immunostaining, Abcam, ab6563, [GR274558-28]

biotin-XX isolectin GS-IB4 conjugate; used in immunostaining, Invitrogen, I21414

biodin-AX isolectin GS-164 conjugate; used in immunostaining, invitrogen, i.

rat anti-mouse CD45; used in cell isolation, BD, BD550539, [8002547] rat anti-mouse CD31; used in cell isolation, BD, BD553369, [0156461]

Dinabeads sheep anti-Rat IgG; used in cell isolation, Invetrogen, 11035, [00862456]

peroxidase-conjugated AffiniPure goat anti-mouse IgG (H+L); used in western blotting, Jackson ImmunoResearch, 115-035-003 peroxidase-conjugated AffiniPure goat anti-rabbit IgG (H+L); used in western blotting, Jackson ImmunoResearch, 111-035-003, [150783]

peroxidase-conjugated AffiniPure donkey anti-goat IgG (H+L); used in western blotting, Jackson ImmunoResearch, 705-035-147, [53331]

#### Validation

anti-human GPNMB antibody(Cell Signaling, #13251); validated to detect human GPNMB for use in western blotting stated on the manufacturer's website.

anti-human GPNMB antibody(Abcam, ab175427); validated to detect human GPNMB for use in immunohistochemistry stated on the manufacturer's website.

anti-human p53 antibody (Santa Cruz, sc-126); validated to detect human p53 for use in western blotting stated on the manufacturer's website.

anti-human p21 antibody (Abcam, ab7960); validated to detect human p21 for use in western blotting stated on the manufacturer's website.

anti-human p16 antibody (BD, 554079); validated to detect human p16 for use in western blotting stated on the manufacturer's website.

anti- $\beta$  actin antibody (Cell Signaling, #4970); validated to detect human and mouse  $\beta$  actin for use in western blotting stated on the manufacturer's website.

anti-mouse Gpnmb antibody(R&D, AF2330); validated to detect mouse Gpnmb for use in western blotting stated on the manufacturer's website.

anti-mouse p53 antibody (1C12) (Cell Signaling, #2524); validated to detect mouse p53 for use in western blotting stated on the manufacturer's website.

anti-mouse p21 antibody (Carbiochem, OP64-20UG); validated to detect mouse p21 for use in western blotting stated on the manufacturer's website.

anti- $\alpha$ -tubulin antibody (11H10) (Cell Signaling, #2125); validated to detect human and mouse  $\alpha$ -tubulin for use in western blotting stated on the manufacturer's website.

anti-GAPDH antibody (Santa Cruz, sc-20357); validated to detect human and mouse GAPDH for use in western blottingstated on the manufacturer's website.

BV421-conjugated anti-mouse Cd31 antibody (BioLegend, 102408); validated to detect mice 113 for use in flow cytometry stated on the manufacturer's website.

PE/Cy7-conjugated anti-mouse Cd45 antibody (BioLegend, 103114); validated to detect mice I13 for use in flow cytometry stated on the manufacturer's website.

BB700-conjugated anti-mouse Cd11b antibody (BD, 564454); validated to detect mice I13 for use in flow cytometry stated on the manufacturer's website.

BV510-conjugated anti-mouse Cd3 antibody (BioLegend, 100234); validated to detect mice I13 for use in flow cytometry stated on the manufacturer's website.

BV605-conjugated anti-mouse Cd19 antibody (BioLegend, 115539); validated to detect mice 113 for use in flow cytometry stated on the manufacturer's website.

APC/Fire750-conjugated anti-mouse Nk 1.1 antibody (BioLegend, 108752); validated to detect mice 113 for use in flow cytometry stated on the manufacturer's website.

BV650-conjugated anti-mouse F4/80 antibody (BioLegend, 123149); validated to detect mice I13 for use in flow cytometry stated on the manufacturer's website.

Pacific Blue-conjugated anti-mouse Ly-6G antibody (BioLegend, 127611); validated to detect mice 113 for use in flow cytometry stated on the manufacturer's website.

BV785-conjugated anti-mouse Cd14 antibody (BioLegend, 123337); validated to detect mice I13 for use in flow cytometry stated on the manufacturer's website.

BV605-conjugated anti-mouse Cd11c antibody (BioLegend, 117333); validated to detect mice I13 for use in flow cytometry stated on the manufacturer's website.

BV711-conjugated anti-mouse Icam1 (Cd54) antibody (BioLegend, 116143); validated to detect mice I13 for use in flow cytometry stated on the manufacturer's website.

eFluor660-conjugated anti-mouse Gpnmb antibody (eBioscience, 50-5708-82); validated to detect mice 113 for use in flow cytometry stated on the manufacturer's website.

eFluor660-conjugated anti-mouse IgG2ak Isotype control antibody (eBioscience, 50-4321-82); validated to detect mice I13 for use in flow cytometry stated on the manufacturer's website.

goat anti-mouse IgG H+L (Cy5) secondary antibody (Abcam, ab6563); validated to detect mouse IgG for use in immunostaining stated on the manufacture's website

biotin-XX isolectin GS-IB4 conjugate(Invitrogen, I21414); validated to detect endothelial cells for use in immunostaining stated on the manufacture's website

rat anti-mouse CD45 (BD, BD550539); validated to detect mouse CD45 for use in flow cytometory stated on the manufacture's website

rat anti-mouse CD31(BD, BD553369); validated to detect mouse CD31 for use in flow cytometory stated on the manufacture's website

Dinabeads sheep anti-Rat IgG (Invetrogen, 11035); validated to detect rat IgG for use in MACS stated on the manufacture's website peroxidase-conjugated AffiniPure goat anti-mouse IgG (H+L) (Jackson ImmunoResearch, 115-035-003); validated to detect mouse

(IgG (H+L) for use in western blotting stated on the manufacture's website

peroxidase-conjugated AffiniPure goat anti-rabbit IgG (H+L) (Jackson ImmunoResearch, 111-035-003); validated to detect rabbit IgG (H+L) for use in western blotting stated on the manufacture's website

peroxidase-conjugated AffiniPure donkey anti-goat IgG (H+L) (Jackson ImmunoResearch, 705-035-147); validated to detect goat IgG (H+L) for use in western blotting stated on the manufacture's website

#### Eukaryotic cell lines

Policy information about cell lines

Cell line source(s)

Human Umbilical Vein Endothelial Cells (HUVEC) was purchased from Lonza Japan (CC-2517, lot 0000439577).

Authentication

HUVECs were verified by qPCR and immunostaining of CD31, and tube formation assay (Cell Biolabs, Inc.).

Mycoplasma contamination

HUVEC cell line were cirtified to be mycoplasma-negative by Lonza.

Commonly misidentified lines (See ICLAC register)

No commonly misidentified cell lines were used in the study.

#### Animals and other organisms

Policy information about studies involving animals; ARRIVE guidelines recommended for reporting animal research

Laboratory animals

C57BL/6 mice were purchased from SLC Japan (Shizuoka, Japan). The DBA/2J and DBA/2J-Gpnmb+ mice were obtained from the Jackson Laboratory. Mice were maintained in a pathogen-free facility at 20–26 °C, 40-60% humidity, under a 12-h light, 12-h dark regimen. We used both male and female mice for the lifespan experiment. For other experiments, we used male mice from 4-20 weeks of age. Description of research mice used for experiments were also described in the relevant Figure legends and/or Methods.

Wild animals

No wild animals were used in the study.

Field-collected samples

No field collected samples were used in the study.

Ethics oversight

All of the animal experiments were conducted in compliance with the protocol reviewed by the Institutional Animal Care and Use Committee of Niigata University and approved by the Institutional Animal Care and Use Committee of Niigata University and the President of Niigata University.

Note that full information on the approval of the study protocol must also be provided in the manuscript.

#### Human research participants

Policy information about studies involving human research participants

Population characteristics

For immunohistochemistry of human aorta, samples were obtained from patients with or without atherosclerotic diseases who admitted to the Department of Cardiovascular Surgery, Niigata University Medical and Dental Hospital, Japan, and were registered to our biobank between 2015-2019. For qPCR studies analyzing GPNMB, leukocytes were collected from patients with or without atherosclerotic diseases who admitted to the Department of Cardiovascular Medicine, Niigata University Medical and Dental Hospital, Japan, and were registered to our biobank between 2013-2015. A total of 70 unique patients ( age 65.6±10.9, male 75.4%) were analyzed. For qPCR studies analyzing GPNMB in leukocytes, atherosclerotic diseases (AD) group included coronary artery disease (n=33), peripheral artery disease (n=5), and cerebrovascular disease (n=1). The patients characteristics were also shown in Extended data figure 1d.

Recruitment

All the patients hospitalized in the department of cardiovascular medicine in Niigata University medical and dental hospital were recruited into the study. There were no self-selection bias. All the patients have cardiovascular diseases needed to be hospitalized. Thus, healthy individuals were not be assessed.

Ethics oversight

All subjects provided written informed consent prior to participation. The Scientific-Ethics Committees of Niigata University approved the study protocols (protocol number H24-585, 2015-2292, 2017-0102), and the studies were performed in accordance with the Declaration of Helsinki. Donors who provided samples for experiments were anonymous.

Note that full information on the approval of the study protocol must also be provided in the manuscript.

#### Clinical data

Policy information about clinical studies

All manuscripts should comply with the ICMJE guidelines for publication of clinical research and a completed CONSORT checklist must be included with all submissions.

Clinical trial registration

N/A

Study protocol

Protocol number H24-585, 2015-2292, 2017-0102

Data collection

Data for these were collected from biobank generated with samples collected between year 2013-2019 in our department.

#### Outcomes

# nature portfolio | reporting summary

Dual	1150	resea	rch	$\circ f$	con	cern
Duai	use	resea	LCII	OI.	COL	кепп

Policy information about <u>dual use research of concern</u>

, and the second	
Hazards	
Could the accidental, deliberate in the manuscript, pose a threat	or reckless misuse of agents or technologies generated in the work, or the application of information presented to:
No Yes  Public health  National security  Crops and/or livestock  Ecosystems  Any other significant area	
Experiments of concern	
Does the work involve any of the	ese experiments of concern:
Enhance the virulence of a  Increase transmissibility of  Alter the host range of a pa  Enable evasion of diagnost  Enable the weaponization	peutically useful antibiotics or antiviral agents  pathogen or render a nonpathogen virulent  a pathogen  athogen
Plots	
Confirm that:	
The axis labels state the mark	ker and fluorochrome used (e.g. CD4-FITC).
The axis scales are clearly vis	ible. Include numbers along axes only for bottom left plot of group (a 'group' is an analysis of identical markers).
All plots are contour plots wi	th outliers or pseudocolor plots.
A numerical value for number	er of cells or percentage (with statistics) is provided.
Methodology	
Sample preparation	Blood samples were collected from tail vein 7 days after neutralizing antibody injection, washed with PBS, and red blood cell lysis was achieved with an ammonium chloride-based lysing buffer (Pharm Lyse, 555899, BD). Cells were resuspended in FACS buffer (PBS supplemented with 1% FBS and 5mM EDTA) and stained with the following antibodies for 30 min on ice. For isolation of the stromal vascular cell fraction (SVF) from gonadal white adipose tissue, fit was excised, minced, and

digested with digesting solution (0.5U/ml collagen, 0.8U/ml dispase and 1mM CaCls in PBS) for 20 min at 37?. For isolation of cells from aorta, aorta was excised, minced, and digested with digesting solution (1.5U/ml collagen, 2.4U/ml dispase and 1mM CaCls in PBS) for 20 min at 37?. The tissue lysate was subsequently filtered through a nylon mesh (40  $\mu$ m) and red blood cell lysis was achieved with an ammonium chloride-based lysing buffer (Pharm Lyse, 555899, BD). Cells were resuspended in PBS supplemented with 1% FBS and 5mM EDTA and incubated with Fcr blocker (1 μg/million cells in 100 μl, 553141, BD) at 4C for 5 minutes) and stained with the following antibodies and 10μM SPiDER beta Gal (Do-Jin-do, SG02) for 30 min on ice.

Instrument

ID7000, SONY

Software

ID7000 software, version 1.1.0.11041

Cell population abundance

For isolation of the stromal vascular cell fraction (SVF) from gonadal white adipose tissue, fat was excised, minced, and digested with digesting solution (0.5U/ml collagen, 0.8U/ml dispase and 1mM CaCls in PBS) for 20 min at 37?. For isolation of cells from aorta, aorta was excised, minced, and digested with digesting solution (1.5U/ml collagen, 2.4U/ml dispase and 1mM CaCls in PBS) for 20 min at 37?.

Gating strategy

Gating strategies are shown in Supplementary figures.